Palaeontologia Electronica
palaeo-electronica.org

A revision of "*Trinitichelys*" *maini* (Testudinata: Baenidae) and additional material of its new genus from the Lewisville Formation (Woodbine Group, Cenomanian), Texas, USA

Brent Adrian, Heather F. Smith, and Christopher R. Noto

ABSTRACT

New cranial and postcranial (including shell and thin sections) material of the baenid turtle *"Trinitichelys" maini* is described and the species is taxonomically revised and referred to a new genus, *Gehennachelys*. The hypodigm of *G. maini* is expanded to include informative specimens allowing for a more comprehensive morphological understanding and shell reconstruction, as well as more thorough comparisons with confamilials.This taxon is phylogenetically placed at the base of Baenodda. *Gehennachelys maini* comb. nov. lacks a contribution of the posteriormost vertebral scale to the carapace margin and an omega-shaped femoral-anal sulcus, both historically regarded as baenodd synapomorphies, despite showing derived cranial characters for Baenodda. This inconsistency challenges the utility of these traits in diagnosing baenodds and highlights problems in resolving baenid relationships. *Gehennachelys* demonstrates that baenodds evolved as early as the middle Cenomanian, and it likely dispersed to southwestern Appalachia during a regression in the early Cenomanian, becoming the terminal baenid from the eastern North American landmass.

Brent Adrian. Institute of Human Origins, School of Human Evolution and Social Change, 900 S. Cady Mall, Tempe, Arizona, 85287 USA. badrian@asu.edu
Heather F. Smith. Department of Anatomy, 19555 N. 59th Avenue, Midwestern University, Glendale, Arizona 85308 USA. hsmith@midwestern.edu
Christopher R. Noto. Department of Biological Sciences, University of Wisconsin - Parkside, Kenosha, Wisconsin, 53141, USA. noto@uwp.edu

Keywords: Paracryptodira; Baenodda; Arlington Archosaur Site; middle Cretaceous; paleobiogeography

Submission: 8 January 2023. Acceptance: 10 July 2023.

https://zoobank.org/06BB716C-7E07-435E-B18D-14B9A965A588

Final citation: Adrian, Brent, Smith, Heather F., and Noto, Christopher R. 2023. A revision of "*Trinitichelys*" *maini* (Testudinata: Baenidae) and additional material of its new genus from the Lewisville Formation (Woodbine Group, Cenomanian), Texas, USA. Palaeontologia Electronica, 26(2):a28.
https://doi.org/10.26879/1266
palaeo-electronica.org/content/2023/3906-new-baenid-genus-gehennachelys

INTRODUCTION

A major marine transgression in the late Albian formed the Skull Creek Seaway, which bisected North America into the isolated land masses of Laramidia and Appalachia, ending the cosmopolitanism and faunal interchange that characterized the Early Cretaceous (Slattery et al., 2015; Blakey and Ranney, 2018; Noto et al., 2022). This transgression correlates with the depositional hiatus observed in the terrestrial record between the Trinity and Woodbine Groups, during which Texas was mostly inundated (Winkler et al., 1995; Noto et al., 2022). A connection between the separate landmasses was re-established in the central United States during a brief sea level fall during the earliest Cenomanian (Slattery et al., 2015; Scotese, 2021; Noto et al., 2022). The Greenhorn Transgression formed the Western Interior Seaway (WIS) by the middle Cenomanian, and the Woodbine Group formed an extensive delta system along the southwestern flank of Appalachia (Slattery et al., 2015; Blakey and Ranney, 2018; Scotese, 2021; Noto et al., 2022).

Currently, four turtle taxa have been identified from the Lewisville Formation of the Woodbine Group in north-central Texas: an indeterminate trionychid; the stem turtle *Naomichelys; Pleurochayah appalachius* Adrian, Smith, Noto, and Grossman, 2021, the oldest pleurodire known from North America; and an abundant species of baenid turtle, given the name *"Trinitichelys" maini* (Adrian et al., 2019). While the Lewisville Formation baenid is found in close geographic proximity to the older baenid *Trinitichelys hiatti* Gaffney, 1972, which occurred in Texas during the Albian, it differs from that species in various regards, and its referral to the genus *Trinitichelys* has been tentative since its initial description.

Baenidae is a speciose, endemic clade of aquatic, mostly carnivorous freshwater turtles that were widely distributed during most of the Cretaceous and through the Eocene of North America, particularly in Laramidia (Hay, 1908; Gaffney and Hiatt, 1971; Gaffney, 1972; Archibald and Hutchison, 1979; Hutchison, 1984; Brinkman and Nicholls, 1991; Hutchison and Storer, 1998; Holroyd and Hutchison, 2002; Brinkman, 2003; Hutchison, 2004; Lipka et al., 2006; Lyson and Joyce, 2009a, 2009b, 2010, 2011; Sullivan et al., 2013; Holroyd et al., 2014; Lively, 2015, 2016; Joyce and Lyson, 2015; Lichtig and Lucas, 2015, 2016; 2018; Smith et al., 2017; Adrian et al., 2019; Joyce et al., 2020; Lyson et al., 2019, 2021). The only known Appalachian baenids are *Arundelemys dardeni* Lipka, Therrien, Weishampel, Jamniczky, Joyce, Colbert, and Brinkman, 2006, from the Early Cretaceous of Maryland, *Trinitichelys hiatti* from the Albian of Texas, and *Gehennachelys maini* comb. nov. from the Cenomanian of Texas, which is the subject of the current study (Gaffney, 1972; Lipka et al., 2006; Adrian et al., 2019). The lack of younger baenid discoveries in Appalachia suggests that *G. maini* comb. nov. may have been the last member of the clade to occupy the eastern landmass, though this is made uncertain by the rarity of pertinently aged (pre-Santonian) terrestrial strata (Schwimmer, 1997; Brownstein, 2018; Noto et al., 2022). It occupied a temporal interval leading to the dominance of the derived clade Baenodda (comprised of the subfamilies Palatobaeninae and Eubaeninae), beginning in the Campanian (Gaffney, 1972; Gaffney and Meylan, 1988; Brinkman, 2003; Lyson and Joyce, 2009a; Joyce and Lyson, 2015; Adrian et al., 2019; Adrian et al., 2023).

The goal of the current study is to describe and analyze new fossil material of *"Trinitichelys" maini* from the Arlington Archosaur Site (AAS) and nearby Grapevine Lake shoreline, which includes two nearly complete shells as well as cranial, non-shell postcranial, and paleohistological specimens. The phylogenetic coding of the original material used to describe *"Trinitichelys" maini* placed it in an unresolved polytomy with *Hayemys latifrons* Hay, 1908 and *Thescelus* spp., as sisters to the lineage leading to the baenodd clades Eubaeninae and Palatobaeninae (Adrian et al. 2019, figure 8). The current study revises the diagnosis of the new combined taxon, *Gehennachelys maini* comb. nov., resulting in a modified phylogenetic placement within Baenidae.

As anticipated in 2019, the new material provides significant evidence that *"Trinitichelys" maini* belongs to its own genus, which is formally named here. The new binomen, *Gehennachelys maini* comb. nov. is created, representing a turtle that is, according to our phylogenetic analysis, more derived than *Trinitichelys hiatti* and *Lakotemys australodakotensis* Joyce, Rollot, and Cifelli, 2020, but basal to palatobaenines and some eubaenines. The new taxon exhibits most of the derived traits that characterize baenodds, but lacks two diagnostic morphologies of the posterior baenodd shell—namely, an omega-shaped femoral-anal sulcus, and the contribution of vertebral scale 5 to the posterior shell margin (Gaffney and Meylan, 1988; Joyce and Lyson, 2015).

Anatomical Abbreviations

ac= acromion; an= anal scale; ce= cervical scale; cm= condylus mandibularis; ct= cavum tympani; ex= extragular scale; fr= frontal; fst= foramen stapedio-temporale; gu= gular scale; hu= humeral scale; im= inframarginal scale; ISF= interwoven structural collagenous fiber bundles; ju= jugal; ma= marginal scale; mx= maxilla; or= orbit; pa= parietal; pe= pectoral scale; pl= pleural scale; pm= premaxilla; po= postorbital; pr= prootic; qj= quadratojugal; qu= quadrate; so= supraoccipital; sq=squamosal; ve= vertebral scale.

Institutional Abbreviations

AMNH, American Museum of Natural History, New York, New York, U.S.A.; DMNH, Perot Museum of Science and Nature (formerly Dallas Museum of Natural History), Dallas, Texas, U.S.A.; HMNS, Heard Natural Science Museum and Wildlife Sanctuary, McKinney, Texas, U.S.A.; USACE, United States Army Corps of Engineers, Dallas, Texas, U.S.A.

GEOLOGICAL SETTING

Lewisville Formation of the Woodbine Group

The Woodbine Group (Gp.) in Texas has a complex and lengthy history of discovery, including differing interpretations and nomenclature based on analyses of surface exposures, subsurface drill cores, wireline logs, and many revisions of its stratigraphic subdivision (Berquist, 1949; Dodge, 1952, 1968; Oliver, 1971; Murlin, 1975; Trudel, 1994; Ambrose et al., 2009; Hentz et al., 2014; Denne et al., 2016; Noto et al., 2022). The Woodbine Gp. is the oldest Upper Cretaceous unit in the Gulf Coastal Plain and is classified as a third order regressive sequence deposited over approximately 1.5 million years (Ambrose et al., 2009; Noto et al., 2022). The surface exposures of the Woodbine Gp. form a narrow, irregular band that extends from Lake Texoma in southern Oklahoma to Temple in central Texas (Dodge, 1969; Oliver, 1971; Johnson, 1974; Trudel, 1994; Noto et al., 2022). In the study area, the Woodbine Gp. sits at an unconformable boundary above the Grayson Marl (Washita Gp.) and is capped by another unconformity with the Eagle Ford Gp. (Denne et al., 2016; Noto et al., 2022) (Figure 1A). A period of marine deposition lasting at least 10 million years separated the Woodbine Gp. from older terrestrial units of the Lower Cretaceous Trinity Gp. (Winkler et al., 1995; Noto et al., 2022) (Figure 1A).

Stratigraphic subdivision of the Woodbine Gp. has undergone repeated changes due to variability in the number and composition of subunits at different locations (Noto et al., 2022). Two units are currently recognized within the Woodbine Gp.: the lower Dexter Formation (Fm.) representing marginal and marine environments (Berquist, 1949; Dodge, 1952, 1968, 1969; Oliver, 1971; Johnson, 1974; Noto et al., 2022), and the overlying Lewisville Fm., which represents a low-lying coastal plain (Powell, 1968; Oliver, 1971; Main, 2009; Noto et al., 2022). Chronostratigraphic and sequence stratigraphic studies suggest that the Woodbine Gp. is no older than middle-early Cenomanian (Ambrose et al., 2009; Adams and Carr, 2010; Donovan et al., 2015; Vallabhaneni et al., 2016; Noto et al., 2022). The ammonite *Conlinoceras tarrantense* is a zonal marker for the base of the middle Cenomanian, providing an early middle Cenomanian age (approximately 96 Ma) for the Lewisville Fm. and the Tarrant Fm. (base of the Eagle Ford Gp.) (Kennedy and Cobban, 1990; Emerson et al., 1994; Lee, 1997; Jacobs and Winkler, 1998; Gradstein et al., 2004; Noto et al., 2022). However, an age as young as late Cenomanian is suggested by Ambrose et al., (2009), with overall deposition of the Woodbine Gp. possibly ending around 92 Ma.

Arlington Archosaur Site

The Arlington Archosaur Site (AAS) is a Lewisville Formation (Fm.) locality in Tarrant County that represents a transition from freshwater or brackish wetlands to near-shore marine environments (Noto, 2015; Noto et al., 2022) (Figure 1). Exposures comprise organic-rich shale (peat), dominated by carbonized plant matter and overlain by gray mudstone-dominated paleosols with abundant charcoalified plant remains and calcareous nodules, followed by an oxidized coarse sand/pebble conglomerate, then interbedded fine sand and silty clay, and capped by rippled sand beds (Noto, 2015; Noto et al., 2022). The AAS has produced a diverse fossil assemblage that includes vertebrates, invertebrates, and plants (Main et al., 2011; Noto et al., 2012; Noto, 2015; Main, 2013; Main et al., 2014; Adams et al., 2017; Adrian et al., 2019, 2021; Noto et al., 2019, 2022) (Table 1).

In particular, all four previously listed turtles known from the Lewisville Fm. were discovered at the AAS (Adrian et al., 2019, 2021). The primary fossil quarry at the AAS was located in the lowermost Facies A and contained the majority of specimens recovered to date (Noto 2015, figures 6-7). It

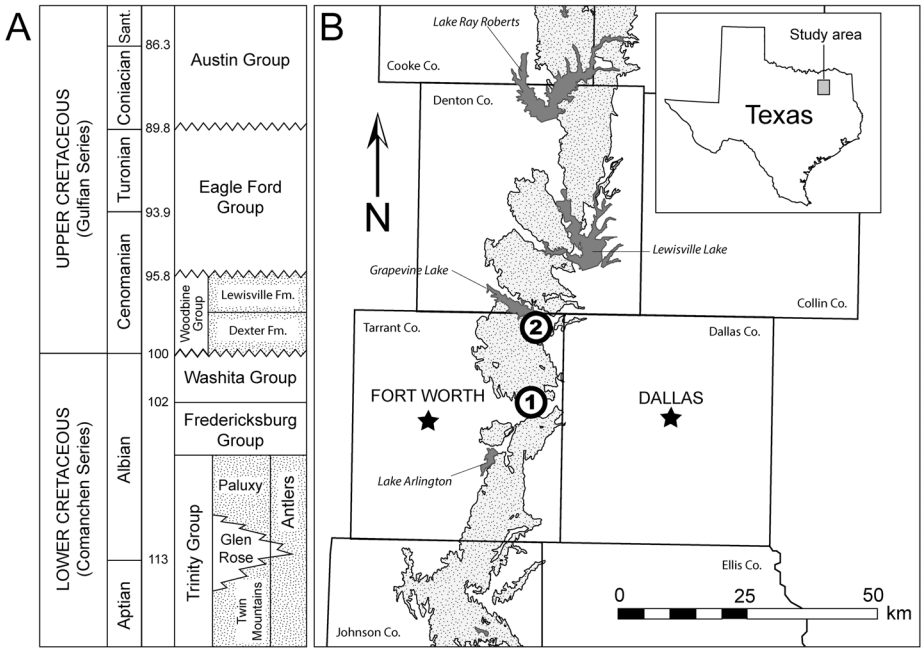

FIGURE 1. Location and geologic position of the Woodbine Group. A, General stratigraphic sequence and timescale for the Cretaceous of central and north central Texas showing the position of the Woodbine Group. Terrestrial deposits represented by stippled intervals. Time scale based on Gradstein et al. (2004) and Denne et al., 2016, and modified from Noto et al. (2022). B, Map of Woodbine surface exposures in the study area showing position of localities where fossils were discovered. Exposures are stippled, water bodies are solid gray. 1 = Arlington Archosaur Site, 2 = Grapevine Lake southwest shore.

is composed of a dark brown sandy siltstone at least 50 cm thick, overlain by a dark gray carbonaceous sandy siltstone measuring 30-40 cm, the upper portion of which contains slickensides, sulfur bands, gypsum, and pyrite (Noto, 2015). Facies A preserves abundant plant material with a high abundance of terrestrial palynomorphs (Main, 2013). In addition to the palynomorphs and well-preserved microscopic organics, rare dinoflagellates, absent foraminifera, lungfish toothplates, lissamphibians, and mostly non-marine or brackish turtles indicate fluvial deposition with minor marine input (Main, 2013; Noto, 2015; Adrian et al., 2021). Fragmentary remains of elasmobranchs and osteichthyans, some indviduals of which are estimated to exceed a meter in length, suggest the presence of nearby deeper water (Noto, 2015). Invertebrates, consisting mainly of shells, represent a mixture of freshwater and brackish groups (Main, 2013). Facies A is interpreted as a low-energy freshwater or brackish system, such as a tidal coastal wetland proximal to a river channel (Rabenhorst, 2001; Noto et al., 2015).

Grapevine Lake Southwest Shoreline near Oak Grove Park

Grapevine Lake is oriented northwest-southeast between and north of Dallas and Fort Worth, Texas (Figure 1B), with extensive Woodbine Group exposures along its shores, including near the spillway associated with the dam (Jacobs et al., 2013, figure 5; Noto 2015, figure 5; Noto et al., 2022) (Figure 1B). It is located in the far northeast corner of Tarrant County, on public land administered by the United States Army Corps of Engineers (USACE) (Noto, 2015). In 1952, the USACE dammed Denton Creek, a tributary of the Elm Fork of the Trinity River, for flood control and as a water source for the Dallas-Fort Worth Metroplex (Jacobs et al., 2013). The Dam Spillway exposure belongs to the Lewisville Fm. based on the presence of *Ostrea*-like oysters and is consistent with a transitional shoreline or near-shoreline setting in a coastal plain environment (Tykoski and Fiorillo, 2010). Most of the outcrop consists of almost featureless, gray, marine mudrock with an occasional thin, reddish, iron-cemented bed that contains invertebrate tracings and borings (Tykoski and Fiorillo, 2010). Fossils recovered from the Dam Spillway deposits include the enantiornithine

TABLE 1. Vertebrate faunal list of the Arlington Archosaur Site. Data from Noto (2015), Adams et al. (2017), Adrian et al. (2019, 2021), and Noto et al. (2019, 2022).

Chondrichthyes	
	Hybodontidae indet.
	Cretodus sp.
	Squalicorax sp.
	Onchopristis dunklei
	Pseudohypolophus (Hypolophus) mcnultyi
	Pseudomyledaphus sp.
Osteichthyes	
	Melvius sp.
	Elopomorpha indet.
	Coelodus sp.
	Enchodus sp.
	Lepisosteidae indet.
Osteichthyes – Dipnomorpha	
	Ceratodus carteri
Amphibia	
	Caudata indet.
	Cryptobranchidae indet.
	Anura indet.
Reptilia – Dinosauria – Theropoda	
	Tyrannosauroidea indet.
	Carcharodontosauria indet.
	Ornithomimosauria indet.
	Dromaeosauridae indet.
	Troodontidae indet.
	Coelurosauria indet.
Reptilia – Dinosauria – Ornithopoda	
	Protohadros byrdi
Reptilia – Crocodyliformes	
	Deltasuchus motherali
	Scolomastax sahlsteini
	Woodbinesuchus byersmauricei
	Terminonaris cf. *robusta*
	Eusuchia indet.
Reptilia – Testudinata	
	Naomichelys sp.
	Gehennachelys maini, comb. nov.
	Pleurochayah appalachius
	Trionychidae indet.
Mammalia	
	Multituberculata indet.

Flexomornis howei, considered the oldest bird in North America, as well as remains of a coelurosaurian theropod and the ornithopod *Protohadros* (Main, 2005; Noto, 2015; Noto et al., 2022). Additional remains of chondrichthyans, osteichthyans, turtles, and crocodyliforms have also been recovered, as well as theropod and hadrosaur tracks (Tykoski and Fiorillo, 2010; Noto, 2015). Geological and palynological work is ongoing at the Dam Spillway, and surface collection of fossils continues.

HMNS-10-TM was discovered near Oak Grove Park, on the southwest shore of Grapevine Lake, across the lake from a stratigraphically measured sequence between Murrell Park and Rock Ledge Park (Main, 2005). Shoreline and water level conditions were not recorded at the time of its excavation, but the discovery site is comprised of fine red sandstone beds of unknown thickness. The water in this area is shallow near the shoreline with extensive emergent vegetation. The exposed area is flat, prone to inundation, and covered by modern soils with established terrestrial vegetation.

The measured stratigraphic sequence on the north shore preserves a nearly complete delta sequence from Grapevine Lake exposures (Main, 2005, 2013), ranging from fluvial channel sands (GP-8 TO GP-10) at Murrell Park, to delta front sands and prodelta muds near Rock Ledge Park (section GP-1) (see stratigraphic description in Main, 2005). Though the discovery site of HMNS-10-TM is on the opposite side of the lake, it is less than 2500 m away. If the conditions are similar on both sides of the lake, the red sandstone beds at the discovery site may correspond with a trough cross-bedded red sandstone at the top of sections GP-8 to GP-10 (Main, 2005). The wavy-ripple laminated arenaceous sand bed is divided by a thin iron concretionary bed and is interpreted as a third order fluvial channel sequence that represents medium term variation in hydrodynamic conditions, belonging to the lower Arlington Member of the Woodbine Formation (Main, 2005, 2013; Noto, 2015). Though the depositional model of the Grapevine Lake exposures may be similar between the measured stratigraphy and the discovery site of HMNS-10-TM, there is a possibility for a significant margin of error.

MATERIALS AND METHODS

History of Recovery and Preparation of *Gehennachelys maini* comb. nov. Shells

DMNH 2013-07-1942, colloquially the “Flying Turtle”, was affectionately named after its jacket

was accidentally ejected from a field vehicle during transport from the Arlington Archosaur Site to the University of Texas at Arlington in 2010. Led by Patrick and Margie Kline, volunteer preparators were able to painstakingly reconstruct almost the full shell of the specimen and its associated skull and postcrania. In order to accomplish this, they created grid-coordinate in situ maps of four portions of the specimen: carapace, plastron, skeleton, and surrounding matrix. They used these maps (scaled down versions of traditional quarry excavation maps) to label each individual fragment and reconstruct the majority of the specimen (Kline et al., 2012). The final result is a nearly complete shell that is missing only the marginal portion of the right anterolateral side and the anterior plastral lobe. Butvar B-76 and Paraloid B-72 were used as adhesives and consolidants for fragile bone, and additional patches of fiberglass cloth were added for additional reinforcement. The prepared shell is stored in two double sided jackets for the separate carapace and plastron, which allow easy access to both sides of the elements.

HMNS-10-TM was discovered near Oak Grove Park on the southwestern shoreline of Grapevine Lake in April 2019 by 9-year-old Ty Leslie Goble. Like DMNH 2013-07-1942, HMNS-10-TM was prepared by volunteers (this time at the Heard Natural Science Museum) under the direction of Patrick and Margie Kline.

Histological Methods

For histological thin-sectioning, costals of DMNH 2013-07-1703 and DMNH 2013-07-0588 were left undecalcified and embedded in plastic resin following the protocol of Lee and Simons (2015). Slides were imaged using a motorized light microscope (Ni-U; Nikon, Tokyo, Japan, USA) with a strain-free long working distance objective (10× Plan Fluor: numerical aperture of 0.3, resolvable size ≈ 1 µm). Focus and stitching of histological montages were controlled by software (NIS Elements D; Nikon, Tokyo, Japan, USA). The montages were sharpened using Photoshop CC (Adobe Inc., San Jose, California, USA), with the "Unsharp Mask" filter set at 10 px, and are high resolution (2.1 µm per pixel).

Documentation of Fossil Material

Fossil specimens were measured with 6″ Mitutoyo Absolute Digimatic calipers to the nearest 0.01 mm and rounded to the nearest 0.1 mm. Angles and some distances were measured from high quality digital photographs using ImageJ (Rasband, 1997-2018). Figures were created with Illustrator CC and Photoshop CC (Adobe Inc., San Jose, California, USA). We apply the taxonomic scheme of turtles presented by Joyce (2007, 2017), and adhere to the phylogenetically defined clades established in PhyloCode guidelines unless otherwise specified (see Laurin et al., 2005; Joyce et al., 2021). Following Hutchison and Bramble (1981) and most modern authors, the two pairs of scales present on the anterior plastron are termed gular and extragular scales, where the gulars are anteromedial to the extragulars and both sets of scales are anterior to the entoplastron.

Phylogenetic Methods

We used as a starting point 105 characters from the baenid matrix of Rollot et al. (2022b), updated to include *Edowa zuniensis* Adrian, Smith, Kelley, and Wolfe, 2023. *Proganochelys quenstedti* Baur, 1887, was included as the outgroup. Following Rollot et al. (2022b), 22 characters were treated as ordered: characters 5, 9, 13, 15, 17, 25, 26, 29, 32, 37, 38, 39, 44, 46, 58, 61, 78, 86, 93, 95, 96, and 99. All phylogenetic analyses were performed using Tree Analysis using New Technology TNT v1.6 (Goloboff and Morales, 2023). A traditional heuristic search was conducted using a tree bisection reconnection swapping algorithm consisting of 1000 Wagner tree replicates. Rogue taxa were identified for exclusion using the "pruned trees" function of TNT. Finally, a 50% majority-rule consensus tree and strict consensus tree of all minimum length topologies were generated. Consistency index (CI) was calculated by dividing the minimum number of possible changes in the tree by the actual number of steps in the minimum length trees. Retention index (RI) was calculated by dividing (maximum steps – observed steps) by (maximum steps – minimum steps). Character optimization was performed using the Common Synapomorphies functions in TNT.

SYSTEMATIC PALEONTOLOGY

BAENIDAE Cope, 1873 (*sensu* Joyce, Parham, Anquetin, Claude, Danilov, Iverson, Kear, Lyson, Rabi, and Sterli, 2021)

GEHENNACHELYS gen. nov.

zoobank.org/322E9DA4-BFA6-48BE-9FC3-3E6D9B6E3A41

Etymology. *Gehenna* refers to the biblical lake of fire and brimstone, connoting the sulphur content in the deposits where the holotype was discovered, and the massive wildfires that were prevalent in the

area during the Cenomanian. *Chelys* is Ancient Greek meaning “turtle”.

Type species. *“Trinitichelys” maini* Adrian, Smith, Noto, and Grossman, 2019.

Diagnosis. Same for the type species, *Gehennachelys maini* comb. nov.

Gehennachelys maini comb. nov. (Adrian et al., 2019)
Figures 2-7

v. 2012 Noto, Main, and Drumheller, figures 2, 4A

v. 2015 Noto, figure 10A, C, E

v. 2019 Adrian, Smith, Noto, and Grossman, figures 2-3

Holotype. DMNH 2013-07-0712, an anterior plastral lobe (Adrian et al. 2019, figure 3.1-4).

Type strata and locality. Upper Cretaceous (early middle Cenomanian) Lewisville Formation, Woodbine Group (Denne et al., 2016). The Arlington Archosaur Site, city of Arlington, Tarrant County, Texas. Exact locality data are on file at the Perot Museum of Nature and Science, Dallas, Texas.

Referred material. See hypodigm of Adrian et al. (2019), and additionally: DMNH 2013-07-1942, a nearly complete shell and cranium with associated postcrania; HMNS-10-TM, a complete shell; DMNH 2013-07-0784, a partial carapace with well preserved sulci; DMNH 2013-07-1431, right coracoid; DMNH 2013-07-0601, right scapula; DMNH 2013-07-1924, second cervical vertebra; DMNH 2013-07-1369, partial right scapula; DMNH 2013-07-0681, partial left scapula and associated bone fragments; DMNH 2013-07-0533, partial left scapula; DMNH 2013-07-2005, partial right scapula.

Distribution. Cenomanian of north central Texas.

Revised diagnosis. The newly combined taxon is diagnosed by the following unique combination of characters, rather than particular autapomorphies: deep upper temporal emargination exposing the anterior margin of the otic chamber in dorsal view; absent parietal-squamosal contact; elongated squamosal processes; prominent crista supraoccipitalis that is not covered anteriorly by the parietals; shell co-ossified in adults, with robust bridge peripherals and absent fenestrae; gular and extragular scales paired and similarly sized, with midline extragular contact; curved gular-extragular sulci; single, undivided cervical scale that is wider than long; straight femoral-anal sulcus; a complete ring of 12 marginal scales that separate the posteriormost vertebral scale from the carapace margin; scalloped posterior carapace margin; anterior and posterior plastral lobes that are approximately equidimensional.

RESULTS

Cranium of DMNH 2013-07-1942

DMNH 2013-07-1942 includes a partial, dorsoventrally crushed cranium consisting of the skull roof, otic region, and part of the rostrum (Figure 2). The basicranial surface is covered in a hard, unextractable matrix rendering most basicranial morphology of the specimen inaccessible (Figure 2C-D). The probable right acromion, separated from the rest of the scapula, is also embedded in this matrix, further obscuring the basicranial morphology (Figure 2). Given its temporal position, the comparative anatomy section below focuses primarily on Early Cretaceous basal baenids and paracryptodires, also mentioning more derived Late Cretaceous baenids when relevant.

The cranium of *Gehennachelys maini* comb. nov. is crushed and somewhat distorted, yet many morphological details can still be interpreted. The skull is subtriangular in shape (Figure 2A-D). It is longer than it is wide, as in basal baenids such as *Trinitichelys hiatti* (Gaffney, 1972; Rollot et al., 2022b) and *Lakotemys australodakotensis* (Rollot et al., 2022a) and other paracryptodires such as *Pleurosternon bullockii* (Evers et al., 2020) and *Uluops uluops* (Rollot et al., 2021). However, the cranial elongation is primarily the result of extensive squamosal processes, which project posteriorly off a cranium that is otherwise wedge-shaped as in most baenodds (Joyce and Lyson, 2015) (Figure 2A-D). The skull surface is minimally sculptured, although this finding may relate to the depositional environment at the site, which also resulted in minimal sculpturing on the associated shell. No cranial sulci are visible.

Anteriorly, the cranium is gracile unlike the robust, blocky morphology of some basal baenids such as *Lakotemys australodakotensis* (Joyce et al., 2020) and *Arvinachelys goldeni* Lively, 2015, and paracryptodires such as *Uluops uluops* Carpenter and Bakker, 1990 (Lively, 2015; Rollot et al., 2021, 2022a). The rostrum tapers to a point (Figure 2A-B), unlike the rounded anterior margin of *Arvinachelys goldeni* (Lively 2015, figures 1-3). Due to crushing, cheek emargination cannot be directly measured, but the morphology of the left maxilla and jugal suggests deep emargination in this region as in most baenodds (Joyce and Lyson, 2015) (Figure 2A-D).

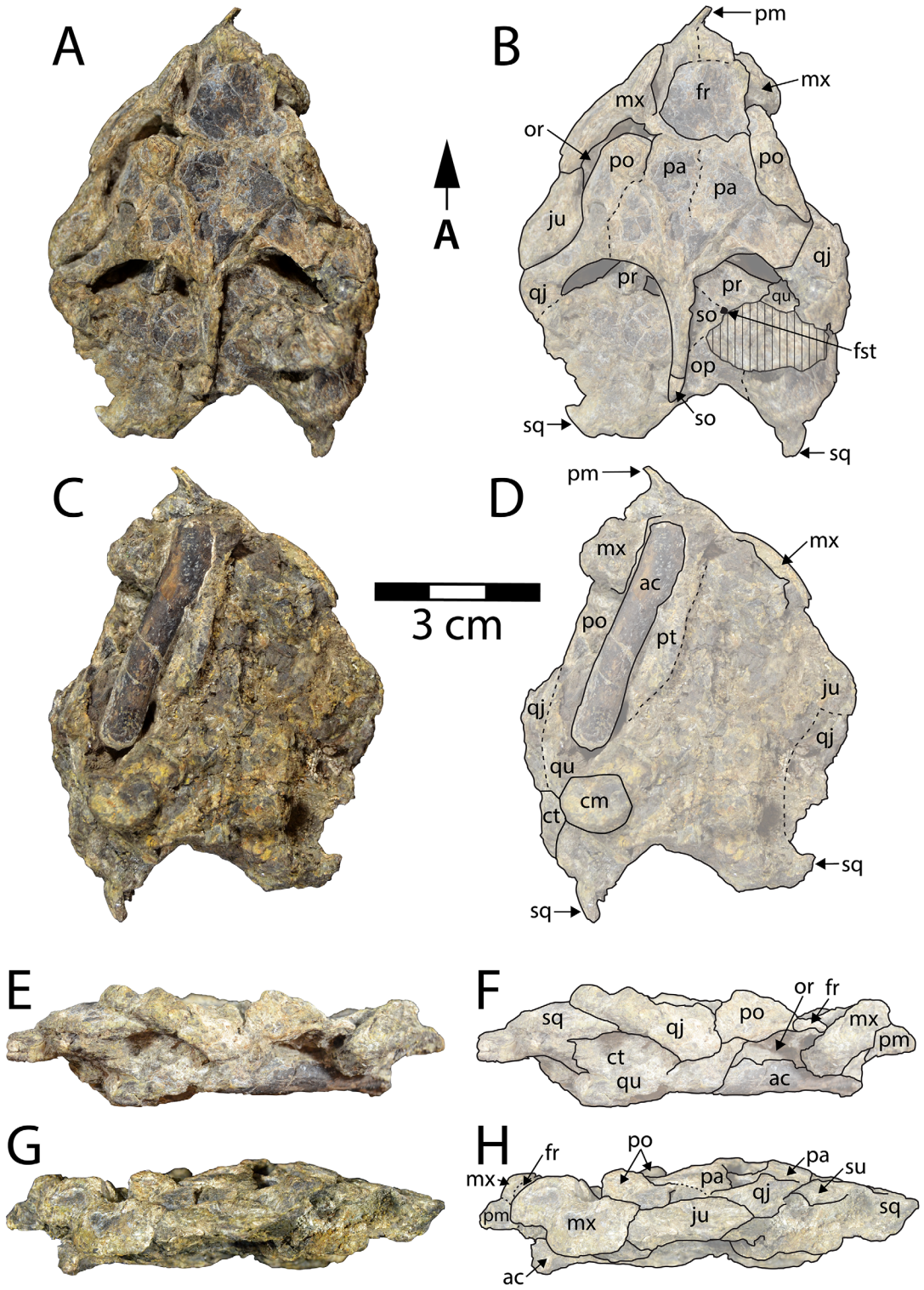

FIGURE 2. DMNH 2013-07-1942, *Gehennachelys maini* comb. nov. skull: A, dorsal photograph; B, dorsal line drawing; C, ventral photograph; D, ventral line drawing; E, right lateral photograph; F, right lateral line drawing; G, left lateral photograph; H, left lateral line drawing. Arrow indicates anterior orientation for A-D. For E and F, anterior is to the right. Abbreviations: ac= acromion; cm= condylus mandibularis; ct= cavum tympani; fr= frontal; fst= foramen stapediotemporale; ju= jugal; mx= maxilla; or= orbit; pa=parietal; po= postorbital; pm= premaxilla; pr= prootic; qj= quadratojugal; qu= quadrate; so= supraoccipital; sq= squamosal.

The parietals comprise the posterior aspect of the skull roof. Each parietal is approximately as wide as it is long (Figure 2A-B), contrasting with the condition in most other baenids, where the parietals are longer than wide. However, the combined width of the parietals exceeds their length in *Trinitichelys hiatti* Gaffney, 1972, *Lakotemys australodakotensis* Rollot et al., 2022a, *Arvinachelys goldeni* Lively, 2015, *Neurankylus lithographicus* Larson et al., 2013, *Hayemys latifrons* (Gaffney, 1972), and the baenodds *Palatobaena cohen* Lyson and Joyce, 2009b, *Stygiochelys estesi* Gaffney and Hiatt, 1971, *Chisternon undatum* (Leidy, 1871a) and *Baena arenosa* Leidy, 1870 (Joyce and Lyson, 2015). The parietals contact the frontals anteriorly, postorbitals laterally, supraoccipital posteriorly, and each other at the midline (Figure 2A-B). There is no parietal-squamosal contact. The frontals form the anterior portion of the skull roof (Figure 2A-B). They are smaller than the parietals as in most baenids, except *Hayemys latifrons* (Gaffney, 1972) and *Arvinachelys goldeni* (Lively, 2015). The frontals are longer than they are wide in *Gehennachelys maini* comb. nov. and are roughly rectangular (Figure 2A-B), as in *Trinitichelys hiatti* (Gaffney, 1972; Rollot et al., 2022b) and most baenodds, and unlike the anteriorly tapering condition in *Lakotemys australodakotensis* (Rollot et al., 2022a) and *Arundelemys dardeni* (Evers et al., 2021). Each frontal contacts the maxilla anterolaterally, postorbital posterolaterally, parietal posteriorly, and its counterpart medially (Figure 2A-F). The frontal-parietal suture is mostly straight. There is no evidence of prefrontal exposure on the skull roof, and while it is possible that this may be the result of taphonomic distortion, there is also very little room between the extensive contacts of the frontals and maxillae. Thus, it seems likely that any possible prefrontal contribution to the skull roof would have been extremely minimal.

Given the relatively short distance between the anterior margin of the frontal and the anterior margin of the rostrum (Figure 2A-B), the nasals are likely to be reduced or absent as in most Baenodda and unlike *Trinitichelys hiatti* (Gaffney, 1972), *Arundelemys dardeni* (Evers et al., 2021), *Hayemys latifrons* (Gaffney, 1972), and *Neurankylus* spp. (Lambe, 1902; Lyson et al., 2016). However, any further details regarding the nasals cannot be definitively evaluated. The postorbitals are elongated but shifted anteriorly out of anatomical position in DMNH 2013-07-1942 (Figure 2A-D). They form the posterior margin of the fossa orbitalis. The postorbital contacts at least the parietal medially, frontal anteromedially, jugal ventrally, and quadratojugal posteroventrally. Due to their bilateral displacement in this specimen, it is not possible to assess any contact between the postorbital and maxilla. The postorbitals contribute to the deep upper temporal emargination. The jugal is present only on the left side, and it contacts at least the maxilla anteriorly and postorbital dorsally (Figure 2A-B). The palatine of DMNH 2013-07-1942 is not preserved, so its possible contact with the jugal cannot be assessed.

The orbits are large, and while their dorsal margins are distorted, it appears that the orbits face laterally as in most baenids (Figure 2A-B, E-F), but unlike many palatobaenine species and *Eubaena cephalica* Hay, 1904 (Hay, 1904; Gaffney, 1972). The jugal contributes to the orbital margin posteriorly, unlike *Arundelemys dardeni* (Evers et al., 2021), *Trinitichelys hiatti* (Rollot et al., 2022b), and several later baenids such as *Eubaena* spp. and *Gamerabaena sonsalla* Lyson and Joyce, 2010 (Hay, 1908; Joyce and Lyson, 2010) (Figure 2A-D). The frontal contributes to the margin of the orbit (Figure 2A-B, E-F), as in most baenids but unlike *Gamerabaena sonsalla*, although the extent of its contribution in an undistorted cranium is unclear (Joyce and Lyson, 2015; Lyson and Joyce, 2010).

The quadratojugal contacts the jugal anteriorly, postorbital dorsally, quadrate posteroventrally, and squamate posterodorsally (Figure 2A-F). It comprises the anterodorsal margin of the large cavum tympani. Portions of both squamosals are preserved, although the bone is more intact on the right side. The squamosal is a conical element, capping the antrum postoticum (Figure 2A-F). It contacts the quadratojugal anteriorly, quadrate anteromedially, and opisthotic posteromedially, and lacks a contact with the parietal. The squamosal forms the posterodorsal margin of the cavum tympani and contributes to the deep upper temporal emargination. The squamosal crests are elongated, projecting posteriorly far beyond the level of the foramen magnum and supraoccipital crest (Figure 2A-B).

The premaxilla projects anteriorly on the left side of DMNH 2013-07-1942 (Figure 2A-F). Its posterolateral contact with the maxilla is the only bony contact preserved. The maxilla is sigmoidal in lateral view, and it comprises the lateral wall of the fossa nasalis, anteroventral margin of the fossa orbitalis, and anteroventral margin of the cheek emargination. It contacts at least the jugal posteriorly, premaxilla anteriorly, and frontal anteriorly

(Figure 2A-F). Due to distortion of the specimen, it is unclear whether the maxilla contacts the postorbital. Similarly, any possible ventral contacts, such as the pterygoid, palatine, or vomer, cannot be assessed.

The quadrate is a large element that forms the condylus mandibularis and most of the cavum tympani. It contacts the quadratojugal anterodorsally, squamosal posterodorsally, prootic anteromedially, supraoccipital medially, and likely opisthotic posteromedially (Figure 2A-F). The ventral surface is largely obscured by matrix, so contacts from this view cannot be assessed. However, the condylus mandibularis is present on the right side, although artificially flattened, and appears moderately sized and oval in ventral view (Figure 2C-D). The prootic is preserved on both sides, but its sutures are largely obliterated. On the right side, it is possible to discern that it contacts the parietal anteromedially, supraoccipital posteromedially, and quadrate posterolaterally (Figure 2A-B). It does not appear to contact the opisthotic, and its possible articulations with basicranial elements such as the pterygoids cannot be assessed. It forms the anteromedial border of the foramen stapediotemporale. The borders of the opisthotic can only be identified on the right side. It contacts at least the supraoccipital anteromedially, squamosal posterolaterally, and likely the quadrate anterolaterally (Figure 2A-B). Any possible contacts with basicranial elements cannot be evaluated. It does not participate in the foramen stapediotemporale. The basicranial region is partly obscured by a bony, cylindrical element that is interpreted to be a right acromion process, which was otherwise unaccounted for (Figure 2C-H). While it is in the general region where a hyoid or hemimandible would be expected, its size, simple cylindrical structure, and lack of articular surfaces or identifiable processes preclude it from being attributed to those elements.

Upper temporal emargination in *Gehennachelys maini* nov. comb is deep with the anterior margin of the otic chamber completely visible in dorsal view (Figure 2A-B). It is deeper than the basal baenids *Trinitichelys hiatti* and *Neurankylus torrejonensis* Lyson, Joyce, Lucas, and Sullivan, 2016 (Gaffney, 1972; Lyson et al., 2016; Rollot et al., 2022b). The squamosal crests are narrow, elongated, and pointed posteriorly (Figure 2), as in *Trinitichelys hiatti* (Gaffney, 1972) but unlike *Lakotemys australodakotensis* (Rollot et al., 2022a) and *Arvinachelys goldeni* (Lively, 2015). There is no contact between the parietal and squamosal (Figure 2A-B), as in baenodds and *Arvinachelys goldeni* (Lively, 2015) and unlike *Trinitichelys hiatti* (Gaffney, 1972; Rollot et al., 2022b), *Lakotemys australodakotensis* (Rollot et al., 2022a), and *Neurankylus torrejonensis* (Lyson et al., 2016).

The cavum tympani is large and dorsoventrally compressed (Figure 2E-F). It is bounded by the quadratojugal anterodorsally, squamosal posterodorsally, and quadrate ventrally (Figure 2A-B, E-F), as in *Lakotemys australodakotensis* (Rollot et al., 2022a), *Uluops uluops* (Rollot et al., 2021), and *Arvinachelys goldeni* (Lively, 2015), and unlike *Palatobaena cohen* (Lyson and Joyce, 2009b) in which the quadratojugal is excluded from the tympanic margin. The remnants of a voluminous antrum postoticum are visible, as in other baenids (Joyce and Lyson, 2015) (Figure 2E-F). The dorsal surface of the otic chamber is abraded and distorted such that very little morphology can be interpreted. However, the right foramen stapediotemporale is visible, positioned dorsally on the otic chamber (Figure 2A-B) as in other baenids (Joyce and Lyson, 2015). The opisthotic is excluded from the foramen stapediotemporale as in most other baenodds and unlike *Lakotemys australodakotensis* (Rollot et al., 2022a), *Trinitichelys hiatti* (Rollot et al., 2022b), and *Stygiochelys estesi* Gaffney and Hiatt, 1971 (Figure 2A-B). The supraoccipital contacts at least the parietals anteriorly, prootics anterolaterally, and opisthotics posterolaterally (Figure 2A-B). Any potential contacts with the quadrate and basicranial elements cannot be assessed in DMNH 2013-07-1942 due to damage. The crista supraoccipitalis is narrow and prominent as it courses dorsally over the otic region (Figure 2A-B). Anteriorly, it is covered only slightly by the parietals as in *Arundelemys dardeni* (Evers et al., 2021) (Figure 2A-B), in contrast to the more extensive coverage seen in most baenids including *Trinitichelys hiatti* (Gaffney, 1972; Rollot et al., 2022b) and *Lakotemys australodakotensis* (Rollot et al., 2022a). Despite distortion in the otic region, it is apparent that the crista supraoccipitalis is short posteriorly (Figure 2A-B). It extends minimally beyond the foramen magnum and does not reach the level of the posterior tip of the squamosals (Figure 2A-B).

Shell of DMNH 2013-07-1942

As mentioned above, the shell of DMNH 2013-07-1942 is nearly complete, only missing the marginal area of the anterolateral section of the carapace and the anterior lobe of the plastron (Figure 3). It was recovered from Facies A of the

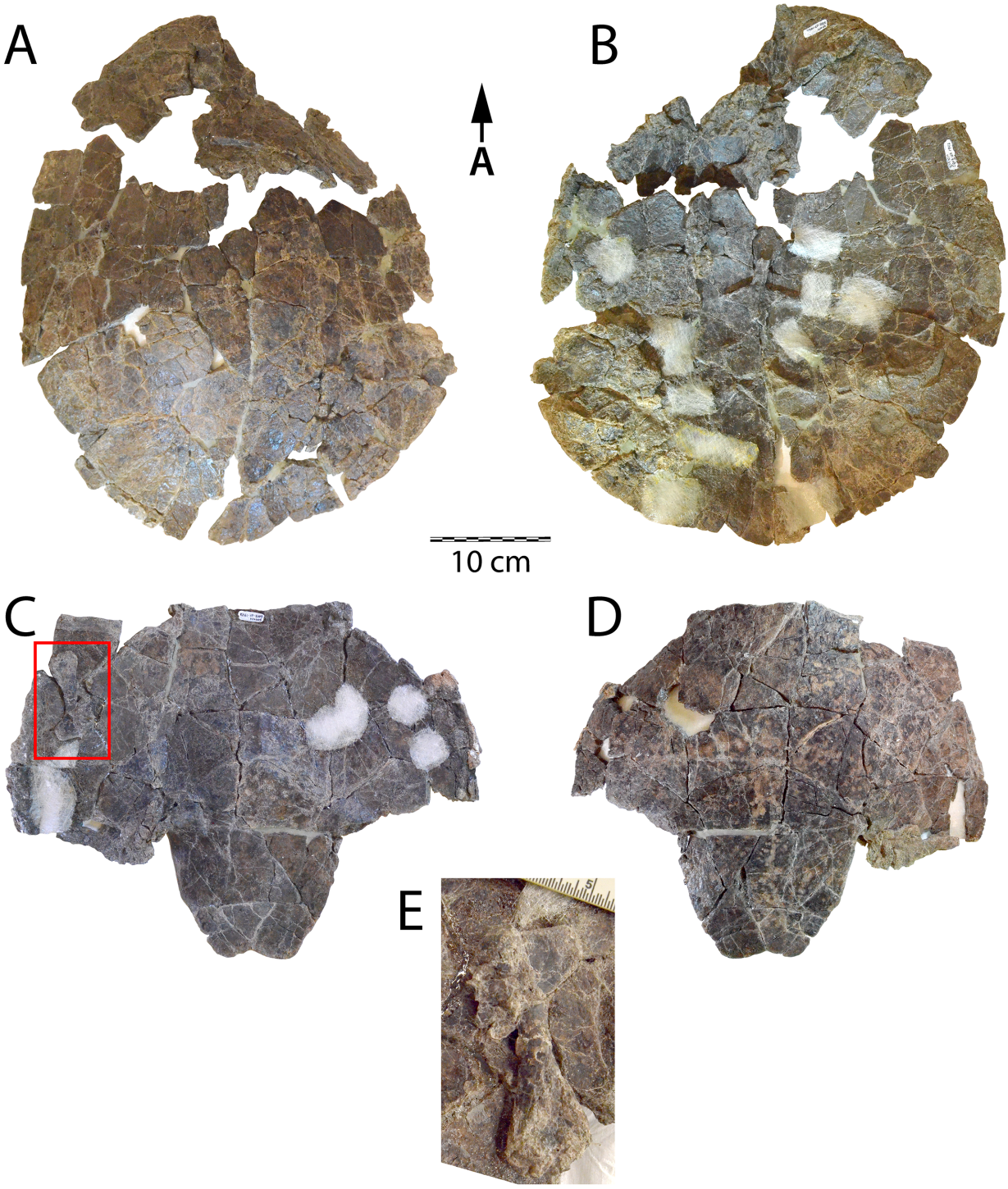

FIGURE 3. DMNH 2013-07-1942 carapace in A, dorsal, and B, ventral views. Plastron in C, dorsal, and D, ventral views. E corresponds with the red box in C, showing the left humerus, rotated 180°. Arrow indicates anterior orientation for A-D. Scale increments in mm for E.

Arlington Archosaur Site. Despite the near completeness of the specimen and its excellent preparation, the superficial surfaces of the shell are poorly preserved (Figure 3). Unfortunately, there is no evidence of sulci, and the number of cracks and instability of most bony components preclude identification of any particular scales. The posterior shell margin is subtly scalloped. The shell rep-

resents an adult individual as evidenced by its complete co-ossification, and no individual bones can be identified. Only small, scattered areas of the external surface are preserved, so little can be ascertained regarding texture of the shell except that it is predominantly smooth. Though relatively complete, the shell of DMNH 2013-07-1942 is badly fractured throughout and crushed flat, eliminating any sense of the natural height of the shell. However, the dorsal base of the left inguinal buttress is preserved (Figure 3B), as well as the ventral base of the right axillary buttress (Figure 3C), showing robust bridge morphology including extensive articulation of the buttresses with costals, as is diagnostic for Baenidae (Lyson and Joyce, 2011; Joyce and Lyson, 2015).

Notably, DMNH 2013-07-1942 has a distinct, moderately developed anal notch (Figure 3C-D). An anal notch was also observed on the juvenile right xiphiplastron DMNH 2013-07-1708 (Adrian et al., 2019: figure 3.18-3.21), however this trait is absent on HMNS-10-TM (Figure 4B). There is also demonstrated intraspecific variability in the nuchal notch. This trait is absent on HMNS-10-TM (Figure 4A, D), not preserved on DMNH 2013-07-1942 (Figure 3A-B), and present, though moderate, on the partial shell DMNH 2013-07-0784 (Adrian et al., 2019: figure 2.1-2.2). On the left side of the ventral surface of the lateral inframarginal region of the plastron, the left humerus is adhered by matrix to the shell surface (Figure 3C, E). Its dorsal surface is visible, and it is oriented in the opposite direction of the shell. The bone is complete except for its proximolateral section and will be considered below with the other postcrania associated with DMNH 2013-07-1942 (Figure 3C, E). In addition, small charcoalified wood fragments were found in the field jacket containing DMNH 2013-07-1942. Small pieces of charcoalified and permineralized wood are prevalent at the AAS as well as the north shore of the Grapevine Lake Dam Spillway, and many coalified remains are preserved as vitrain (Main, 2013; Noto, 2015) (Figure 1B). A particularly large conglomeration of more than 20 coalified tree trunks (0.5–4 m long) was discovered in 2008 near the base of Facies A, the primary vertebrate-bearing layers at the AAS (Main, 2013; Noto, 2015). The trunks were aligned in a northeast-southwest direction and probably represent transported debris (Main, 2013; Noto, 2015).

Shell of HMNS-10-TM

HMNS-10-TM is the most complete and best-preserved shell known of *Gehennachelys maini* comb. nov., and was recovered from the southwest shoreline of Grapevine Lake (Figure 4). The shell is complete and preserves a mostly undistorted, hydrodynamic, natural “teardrop” shape in lateral view, similar to that found in other baenids (*C. undatum* in Gilmore 1915, figure 7; *B. arenosa* in Smith et al. 2017, figure 4) (Figure 4C). HMNS-10-TM allows at least an external view of the intact bridges and formidable buttresses (Figure 4D), which is not afforded by the crushed DMNH 2013-07-1942 (Figure 3). This structural preservation provides a sense of the lateral constriction imposed on the body cavity by the massive buttresses, which could have affected accommodation of the head and limbs in the anterior shell. The posterior plastral lobe is broken off posterior to the base and is displaced and preserved immediately dorsal to the base, overlapping it by approximately 2 cm (Figure 4B-C). A wedge-shaped portion of the left posterolateral side of the dorsal carapace is also broken and displaced dorsally (Figure 4A, E). There is no evidence that the hard, sandstone cast within the shell contains any bones. The shell appears to be completely co-ossified with no apparent sulci, indicating an adult individual (Figure 4).

Despite the completeness of HMNS-10-TM, and similar to the shell of DMNH 2013-07-1942, no sulci or organized texture are visible on the superficial shell surfaces. However, the specimen is unique in its completeness and preservation of the overall shape of the shell. In addition to the taphonomic distortions mentioned above, the center of the plastron is broken and depressed (Figure 4B-D). The fractures in the plastral plate are wide and occur along the midline, approximately the center of the plastron, and near the bases of each lobe (Figure 4B). Much of the deformation is due to crushing, however the center of the plastron appears to have possibly been slightly concave naturally. A concave plastron is sexually dimorphic for males in many turtle taxa, and baenids have been documented to exhibit dimorphic size and plastral morphologies (Lyson et al., 2019). As mentioned above, though the shells of HMNS-10-TM and DMNH 2013-07-1942 share a broadly consistent morphology, the former specimen is lacking both an anal and nuchal notch. In contrast, an anal notch is present in DMNH 2013-07-1942 and DMNH 2013-07-1708, a previously described juvenile specimen; another partial shell (DMNH 2013-07-0784) has a nuchal notch, but the area is not preserved in DMNH 2013-07-1942 (Adrian et al., 2019: figures 2.1-2.2, 3.18-3.21). Though the vari-

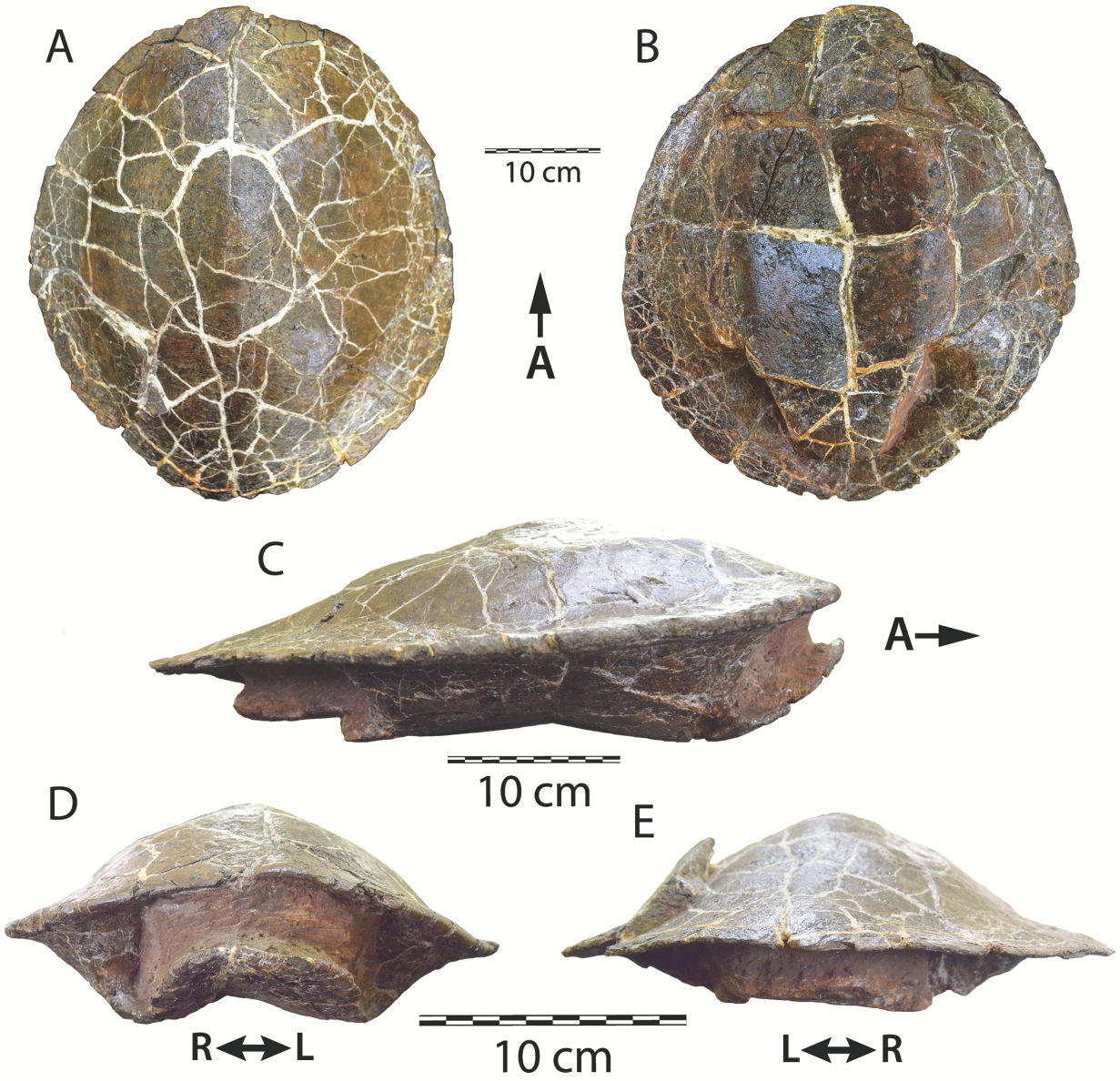

FIGURE 4. HMNS-10-TM, shell of *Gehennachelys maini* comb. nov., in A, dorsal, B, ventral, C, right lateral, D, anterior, and E, posterior views. Note separate scales for A-B, C, and D-E.

ability of the anal and nuchal notches could be due to dimorphism, limited sample size currently hinders a more definitive assessment.

Postcrania of DMNH 2013-07-1942

Vertebrae. Baenid cervical vertebrae are typically anteroposteriorly short and dorsoventrally tall with a distinct ventral keel (Joyce and Lyson, 2015). This condition is consistent with the five cervical vertebrae preserved in DMNH 2013-07-1942 (Figure 5A-C). Concavity and convexity of particular centrum articulations are extremely variable among turtles, and also within Baenidae, although the 4th cervical is typically amphicoelous and the 8th cervical is generally procoelous (Williams, 1950; Lyson and Joyce, 2009a). In *Gehennachelys maini* comb. nov., cervical vertebra 2 is opisthocoelous, as in *Neurankylus eximius* Lambe, 1902 and *Chisternon undatum* (Leidy, 1871a), but unlike *Cedrobaena brinkman* (Lyson and Joyce, 2009a), *Plesiobaena antiqua* (Lambe, 1902), and *Boremys pulchra* (Lambe, 1906) (Lyson and Joyce, 2009a) (Figure 5A-C). It is 17.0 mm long, 13.4 mm wide, and 18.6 mm tall. It does not preserve the prezygapophyses, and is missing its left postzygapophysis, but has a tall neural spine (Figure 5A-C). Its trans-

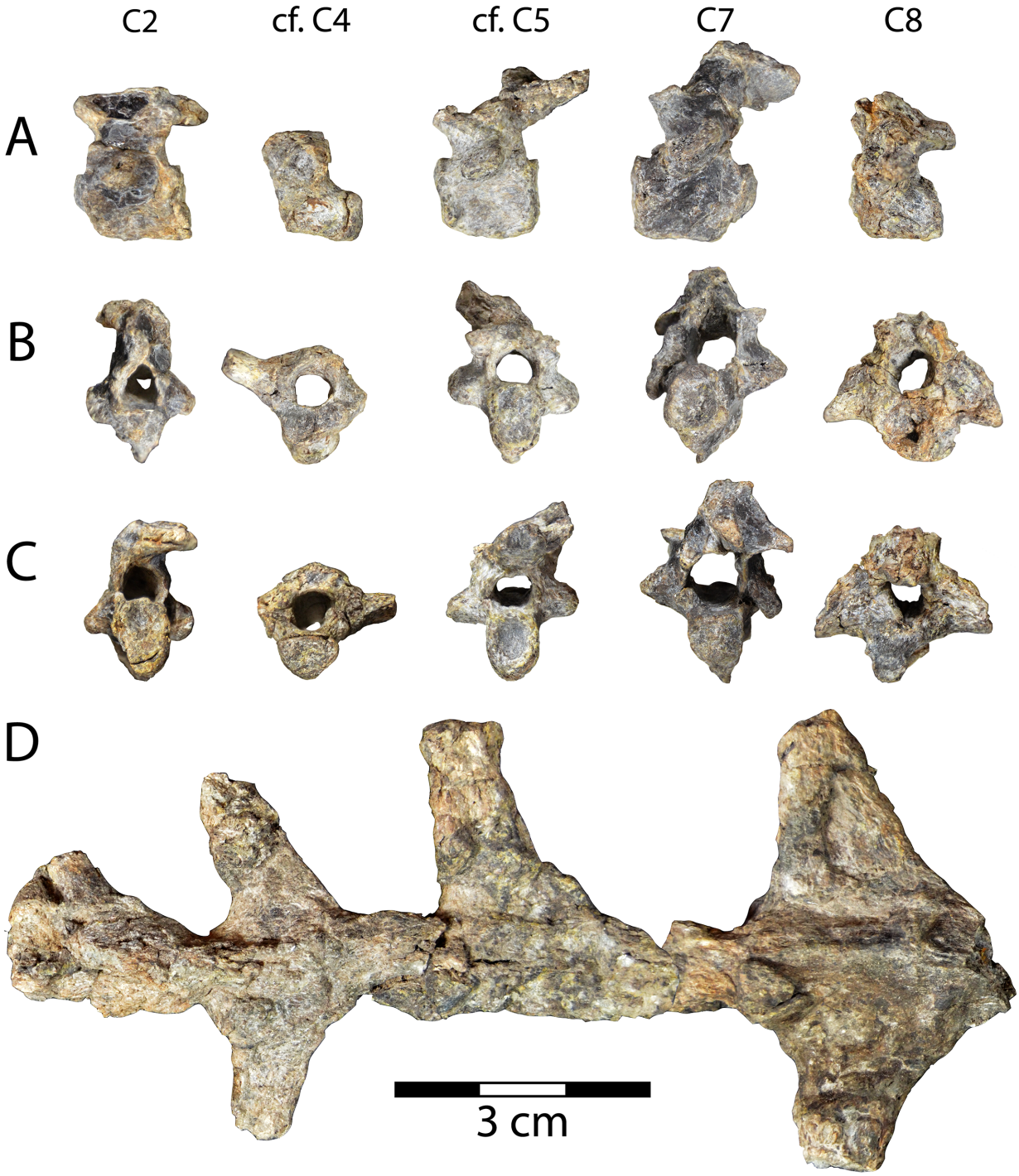

FIGURE 5. DMNH 2013-07-1942 vertebrae. Cervical vertebrae in A, left lateral, B, anterior, and C, posterior views. Ventral view of indeterminate dorsal vertebrae in D, with anterior to the right.

verse processes are short and rounded and project laterally from the middle of the centrum (Figure 5B-C). Its vertebral foramen is approximately triangular, rounded, and taller than wide (Figure 5B-C). There is a ventral keel running the length of the centrum and it contributes to the posterior articular surface, which is taller than wide (Figure 5A, C).

A partial vertebra is tentatively identified as cervical vertebra 4 (Figure 5A-C). Its anterior articulation is concave, and its posterior articulation is flatter, but very slightly concave (Figure 5B-C). Its

articular surfaces are round anteriorly and wider than tall posteriorly (Figure 5B-C). It is missing its left transverse process, and any processes projecting from the neural arch have been broken off (Figure 5A-C). Its intact right transverse process projects approximately 5 mm dorsolaterally from the anterior portion of the centrum and neural arch (Figure 5B-C). The ventral keel is reduced to a ridge running the length of the centrum, which is 8.9 mm long and a maximum of 5.7 mm tall posteriorly (Figure 5A-C). The posterior articular surface of the centrum is larger and wider than the anterior, and the vertebral foramen is round with a 4.8 mm diameter (Figure 5B-C).

Another vertebra, this one complete, is tentatively identified as cervical vertebra 5 (Figure 5A-C). It is 22.7 mm tall, 19.1 mm long, and 15.7 mm wide. Rounded, transverse processes project laterally from the middle of the centrum and measure 5.7 mm wide, 3.7 mm tall, and 3.8 mm long (Figure 5B-C). Its vertebral foramen is approximately circular with a flat bottom, and 4.1 mm in diameter (Figure 5B-C). The centrum is opisthocoelous, although the ventral portion of the anterior articular surface is slightly concave (Figure 5A). Both articular surfaces of the centrum are taller than wide (Figure 5B-C). All other known baenids have fifth cervical vertebrae that are amphicoelous or procoelous (Lyson and Joyce, 2009a). The postzygapophyses are tall and slightly twisted counterclockwise and to the right, and project approximately 5 mm posteriorly beyond the centrum (Figure 5A, C). A ventral keel travels the length of the centrum, becoming taller posteriorly (Figure 5A).

The 7th cervical vertebra is the largest preserved from DMNH 2013-07-1942, measuring 27.3 mm tall, 20.6 mm long, and 16.7 mm wide (Figure 5A-C). It is opisthocoelous, as in *Plesiobaena antiqua* and *Chisternon undatum*, but unlike *Cedrobaena brinkman*, *Neurankylus eximius*, and *Boremys pulchra* (Lyson and Joyce, 2009a) (Figure 5A-C). The articular surfaces of the centrum are taller than wide, and the ventral keel is shortened to a ridge along the length of the centrum (Figure 5A-C). The transverse processes are short, slightly flattened, and tilted anteriorly, originating from the lateral surface of the neural arch just anterior to the middle of the centrum (Figure 5B-C). The postzygapophyses are tall and extend dorsally and posteriorly approximately 3 mm past the centrum (Figure 5A, C). They are distorted slightly clockwise and to the right. The vertebral foramen is significantly larger in the 7th cervical vertebra than the others recovered, measured at 6.7 mm tall and 5.9 mm wide (Figure 5B-C). However, it may be artificially large due to the distortion mentioned above, which also bent the right transverse process ventrally and broke off the right prezygapophysis (Figure 5A-C). The intact left prezygapophysis is short with an anterodorsally oriented articular facet (Figure 5A-B). A triangular ventral keel runs the length of the centrum, and is short anteriorly but becomes taller posteriorly (Figure 5A).

The 8th cervical vertebra of DMNH 2013-07-1942 is missing the prezygapophyses beyond the bases (Figure 5A-C). The bone is 17.7 mm tall, 12.6 mm long, and 21.3 mm wide. It is procoelous, as in baenids generally, except for *Neurankylus eximius* (Williams, 1950; Lyson and Joyce, 2009a). The roof of the neural arch is titled dorsally at its anterior end, to approximately 45° from the centrum (Figure 5A). The transverse processes are aligned with and continuous with the bases of the prezygapophyses (Figure 5A). Viewed anteriorly, the transverse processes are larger than the centrum and triangular, with ventral edges that are perpendicular to the centrum, narrowing dorsally (Figure 5B). The transverse processes project from near the middle of the centrum, and they originate from its entire length (Figure 5A-C). The anterior end of the vertebral foramen is subcircular and approximately 6.4 mm in diameter (Figure 5B). The posterior end of the foramen is slightly smaller, and the posterior end of the centrum is smaller than the anterior (Figure 5C). There is no ventral keel. In general, the cervical vertebrae of *Gehennachelys maini* comb. nov. closely resemble other published baenid cervical series—*Chisternon undatum* (Hay, 1908, figure 83), *Cedrobaena brinkman* (Lyson and Joyce, 2009a, figure 8), and *Neurankylus baueri* Gilmore, 1916 (Lichtig and Lucas, 2018, figures 10-11)—but have generally shorter centra.

Dorsal vertebrae are not well described or figured for baenids. We identify a series of three and a half dorsal vertebrae that articulate with each other, but are separate from the shell, and one vertebra that remains attached to the ventral surface of the carapace (Figures 3B, 5D). The attached vertebra is located near the center of the ventral surface of the carapace, and we infer that the separate series of vertebrae would have been located posterior to it due to the reduction of width that occurs approaching the pelvic girdle (Figure 3B). However, it is not possible to identify the precise vertebrae present. For the separate series, we surmise that the transverse processes become wider anteriorly, and are swept posteriorly in ventral

views (see ventral carapace of *Plesiobaena antiqua* in Brinkman 2003, figure 7). The anteriormost vertebra has a maximum width of 55.0 mm, the next is partial and estimated to be 60 mm wide, and the most posterior has a maximum width of 43.9 mm (Figure 5D). The length of the entire series is 114.7 mm. The vertebra attached to the carapace has a maximum length of 56.5 mm and an estimated maximum width of approximately 57 mm (Figure 3B).

Shoulder girdle and forelimbs. Both scapulae of DMNH 2013-07-1942 are represented, but neither is fully intact (Figure 6A-D). Both are missing their acromial processes, broken off at the bases. The entire length of the left side, including the scapular process is 76.7 mm, and the straight, rod-like scapular process is 6.4 mm in diameter (Figure 6A-B). On the right side, the total length including scapular process is 90.9 mm, and the scapular process is 6.7 mm in diameter (Figure 6C-D). The head of each scapula is approximately triangular proximally and has a larger, slightly concave facet representing the glenoid fossa, and a smaller articular facet for the coracoid (Figure 6A, C). As in many turtles, the scapula and coracoid are triradiate and the glenoid fossa is formed by the scapula anteriorly and the coracoid posteriorly. The scapular necks are short and each has a prominent supraglenoid tubercle (Figure 6A-D). The acromial process of the right scapula is attached to the ventral side of the base of the skull (Figure 2C-D). Like the scapular process, it is straight and columnar. Its broken end is oriented anteriorly and is slightly flattened in cross section, while the apparently intact free end is slightly convex (Figure 2C-D). The bone measures 44.7 mm long and is 7.6 mm wide.

Since neither scapula of DMNH 2013-07-1942 is complete, a more intact right scapula of *Gehennachelys maini* comb. nov., DMNH 2013-07-0601, can provide additional detail (Figure 6E-F). The specimen is extremely well preserved, except the distal portion of its acromion process is cleanly broken off (Figure 6E-F). The total length of the bone including the scapular process is 76.7 mm, and the process is 6.2 mm in diameter. The intact portion of the acromial process is approximately 23.5 mm long from where it meets the scapular neck, and it is 6.1 mm in diameter (Figure 6E-F). The anterolateral side of the scapular neck is slightly concave (Figure 6F), while the opposite side is somewhat convex (Figure 6E). The angle between the acromial and scapular processes of DMNH 2013-07-0601 is approximately 100° (Figure 6E-F). In comparison, the angle between processes of the scapula in *Chisternon undatum* is approximately 125° (Hay 1908, figure 84). The same angle in *Neurankylus baueri* measures 92° (Lichtig and Lucas 2018, figure 22e), 87° in another *N. baueri* specimen (Lively 2016, figure 3B), 96° in *"Baena" affinis* Leidy, 1871b (*Baena riparia* of Hay, 1908) (Hay 1908, figure 61), and 92° in *Glyptops plicatulus* (Hay 1908, figure 20).

Coracoids from both sides are preserved in DMNH 2013-07-1942, however, the left side is missing the head and neck (Figure 6G-J). Therefore, only the complete right side is described here. The maximum length of the bone is 60.1 mm, and the distal blade-like portion has a maximum width of 27.5 mm (Figure 6G-H). The blade is broad and triangular with straight posterior and curved anterior edges (Figure 6G-H). None of the blade exceeds 4 mm in thickness, and the posterior edge of the coracoid is about twice the thickness anteriorly. The neck is thin and reaches 4.7 mm in diameter (Figure 6G-H). Damage to the coracoid head obscures details of the articular surfaces, but the head forms an approximately equilateral triangle that is 13.1 mm wide in proximal view. Unfortunately, few examples of baenid coracoids have been described. Compared to *Neurankylus baueri*, the coracoid of *Gehennachelys maini* comb. nov. is proportionally longer and has a thinner neck and less robust head (Lichtig and Lucas 2018, figures 21G, 22c) (Figure 6G-H). *"Baena" affinis* Leidy, 1871b (*Baena riparia* of Hay, 1908) has a coracoid with a similarly thin neck to *G. maini* nov. comb., but its blade portion is narrower (Hay 1908, figure 62). The coracoid of *Glyptops plicatulus* is generally more robust than *G. maini* comb. nov., with a larger head and thicker neck, though the distal expansion is not as wide (Hay 1908, figure 21).

BBoth humeri of DMNH 2013-07-1942 are preserved, with the right isolated (Figure 6K-P), and the left adhered to the left inframarginal region of the ventral plastron (Figure 3C, E). The right side has previously been figured with two humeri of *Naomichelys* (Noto 2015, figure 10A), and is described and compared here. The right humerus is complete and well preserved, apart from surface damage and some distortion in its distal third (Figure 6K-P). It is 77.7 mm in total length, and the proximal portion of the bone has a maximum proximal width of 35.2 mm. The humerus is similar to other turtles, in that the proximal and distal expansions are in almost the same plane, and the shaft has a sigmoidal curve visible in anterior and posterior views (Gaffney, 1990) (Figure 6K-P). The diameter of the midshaft is 8.3 mm. The lateral

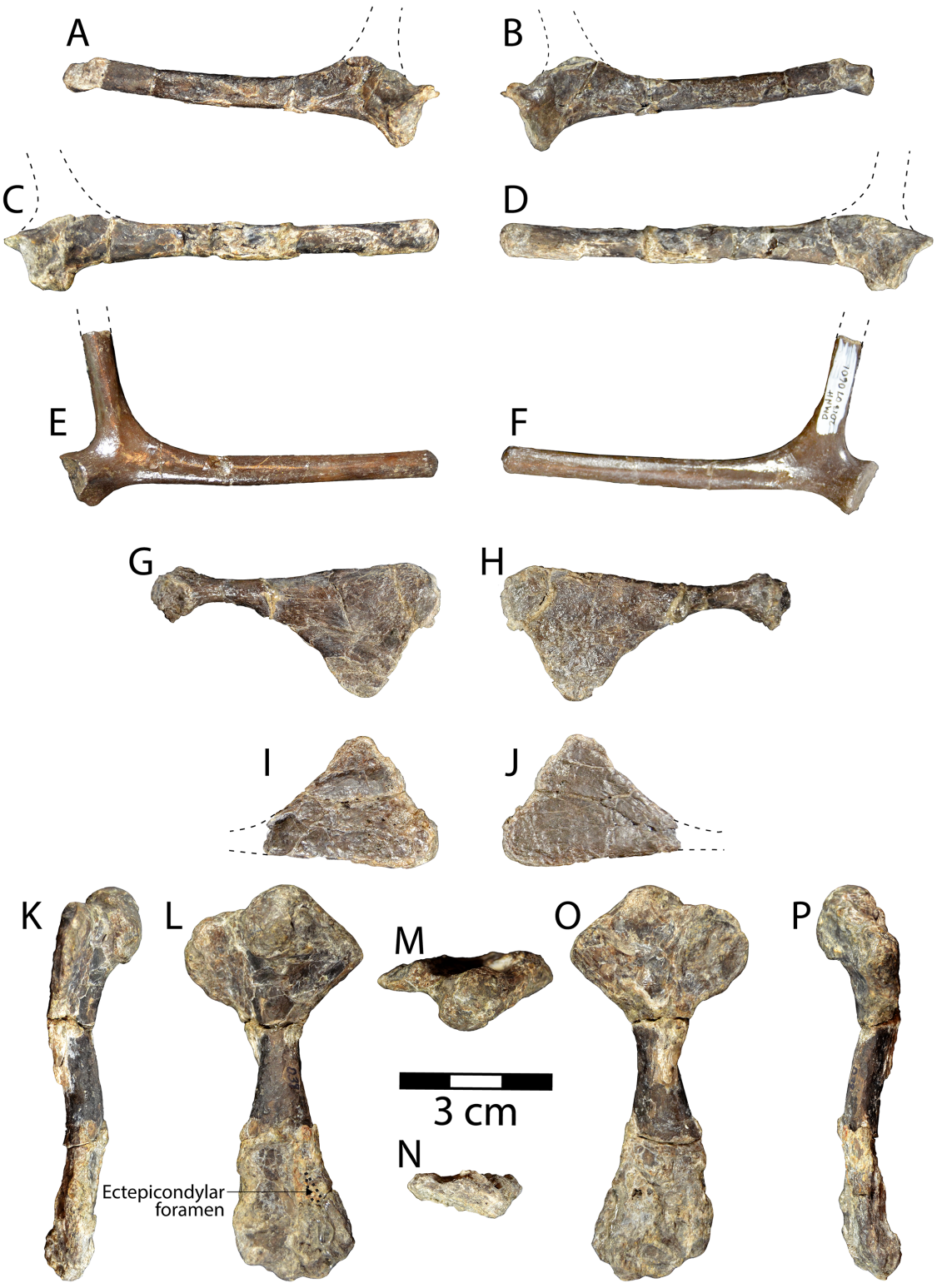

FIGURE 6. DMNH 2013-07-1942, *Gehennachelys maini* comb. nov. shoulder girdle and forelimb bones. Partial left scapula of DMNH 2013-07-1942 in A, posteromedial, and B, anterolateral views. Partial right scapula of DMNH 2013-07-1942 in C, posteromedial, and D, anterolateral views. Partial right scapula of DMNH 2013-07-0601 in E, posteromedial, and F, anterolateral views. Right coracoid of DMNH 2013-07-1942 in G, dorsal, and H, ventral views. Partial left coracoid of DMNH 2013-07-1942 in I, dorsal, and J, ventral views. Right humerus in K, posterior, L, dorsal, M, proximal, N, distal, O, ventral, and P, posterior views. M and N are oriented with B.

(anterior) and medial (posterior) of the proximal humeral expansion are prominent and asymmetrical, with the medial process semicircular and the lateral process triangular when viewed dorsally (Figure 6L-M, O). As in many cryptodires, the anterior side of the proximal expansion has a distinct, sloping shoulder connecting the caput humeri and the lateral process (Gaffney, 1990) (Figure 6L, O). The deltopectoral crest is distinct, connecting the distal end of the caput humeri to the tip of the lateral process (Figure 6L). The caput humeri is hemispherical and nearly round when viewed dorsally, measuring 15.0 mm long and approximately 15.1 mm wide (Figure 6L). Ventrally, the intertubercular fossa is C-shaped, concave and shallow (Figure 6O). The caput humeri extends proximally past either process and is somewhat compressed dorsa-ventrally, measuring 13.0 mm (Figure 6K-L, O-P). The distal humerus appears similar to most turtles in having a flattened, double condyle, with the larger ectepicondyle located on the anterior side, and the smaller and shorter entepicondyle positioned posteriorly (Gaffney, 1990) (Figure 6L, N, O). There is a ~3 mm diameter depression on the dorsal side of the ectepicondyle, which may correspond with the ectepicondylar foramen (Figure 6L). However, it is unclear whether this depression represents a groove or fully formed foramen, as its development varies in turtles (Gaffney, 1990). Damage in the area prevents further definitive description.

The humerus is known from several other, mostly relatively basal, baenid taxa. The humerus of *Gehennachelys maini* comb. nov. is similar to that of *Baena arenosa* except that the proximal extent of both the lateral and medial processes in the latter are turned proximally and both processes extend proximally beyond the caput humeri (Hay 1908, figure 47). The medial process of *Neurankylus hutchisoni* (Hutchison et al., 2013) is also taller than the caput humeri, unlike *G. maini* comb. nov., but its lateral process is similar in shape and position (Lively 2016, figure 3C). *Neurankylus torrejonensis* also differs from *G. maini* comb. nov. in that the medial humeral process is larger and approximately as tall as the caput humeri, with a rectangular rather than rounded edge, and the lateral process has a convex rather than straight shoulder (Lyson et al. 2016, figure 5.5; Lichtig and Lucas 2018, figure 15A-C). *Neurankylus torrejonensis* also appears to have a small, but fully formed, ectepicondylar foramen, and a straighter humeral shaft (Lyson et al. 2016, figure 5.4; Lichtig and Lucas 2018, figure 15D-F). The humerus of *"Baena" affinis* Leidy 1871b (*Baena riparia* of Hay, 1908) also differs from *G. maini* comb. nov. in having a medial process taller than the caput humeri, and the shoulder of its lateral process is concave rather than straight (Hay 1908, figures 63-64). The humerus of *Plesiobaena antiqua* (*Baena antiqua* of Russell, 1934) may be damaged, but it resembles *G. maini* comb. nov. with a similar lateral process and a considerably smaller, but similarly low, medial process (Russell 1934, plate 5, figures 1-2). Finally, the humerus of *G. maini* comb. nov. is generally like that of *Glyptops plicatulus*, except the latter, as in all previously compared taxa except *Plesiobaena antiqua*, has a medial process that is as tall as the caput humeri (Hay 1908, figure 22).

The humerus of *Gehennachelys maini* comb. nov. has prominent (especially medial) processes, a slightly curved and relatively gracile humeral shaft, thus occupying a position in the constructed morphospace of Dickson and Pierce (2019) only similar to that of the widespread modern North American emydids *Deirochelys reticularia* (Latreille, 1801) (Chicken Turtle) and *Malaclemys terrapin* (Schoepff, 1793) (Diamondback Terrapin) (Nakajima et al. 2014, figure 3A; Dickson and Pierce 2019, figure 3A, S1). This region of morphospace lies between the majority of modern semi-aquatic turtles (mostly geoemydids and emydids) and trionychids (Dickson and Pierce, 2019). The placement of the *G. maini* comb. nov. near two broadly distributed eastern North American emydids that are isolated from the majority of modern semi-aquatic pan-testudinoids suggests that this baenid and these emydids may have shared a similar ecological niche. Semiaquatic turtles typically have humeri that are functionally adapted for strength, mechanical advantage, stride length, and hydrodynamics in relatively equal measures (see discussion in Dickson and Pierce, 2019).

Pelvic girdle and hind limbs. The right side of the pelvis of DMNH 2013-07-1942 is incompletely preserved, missing much of the pubic and ischial projections (Figure 7A-C). As noted for other postcrania, the pelvis is distorted and its superficial surface is somewhat crumbled and deteriorated (Figure 7A). The ilium, pubis, and ischium are all broken at their necks, but the proximal portions contributing to the acetabulum are well preserved and co-ossified (Figure 7A). The acetabulum is represented by a large, subcircular depression whose rim is generally intact, but damaged (Figure 7A). Also, there is a second concavity on the proximolateral ilium, adjacent to the acetabulum, which is interpreted as the base of a missing protuber-

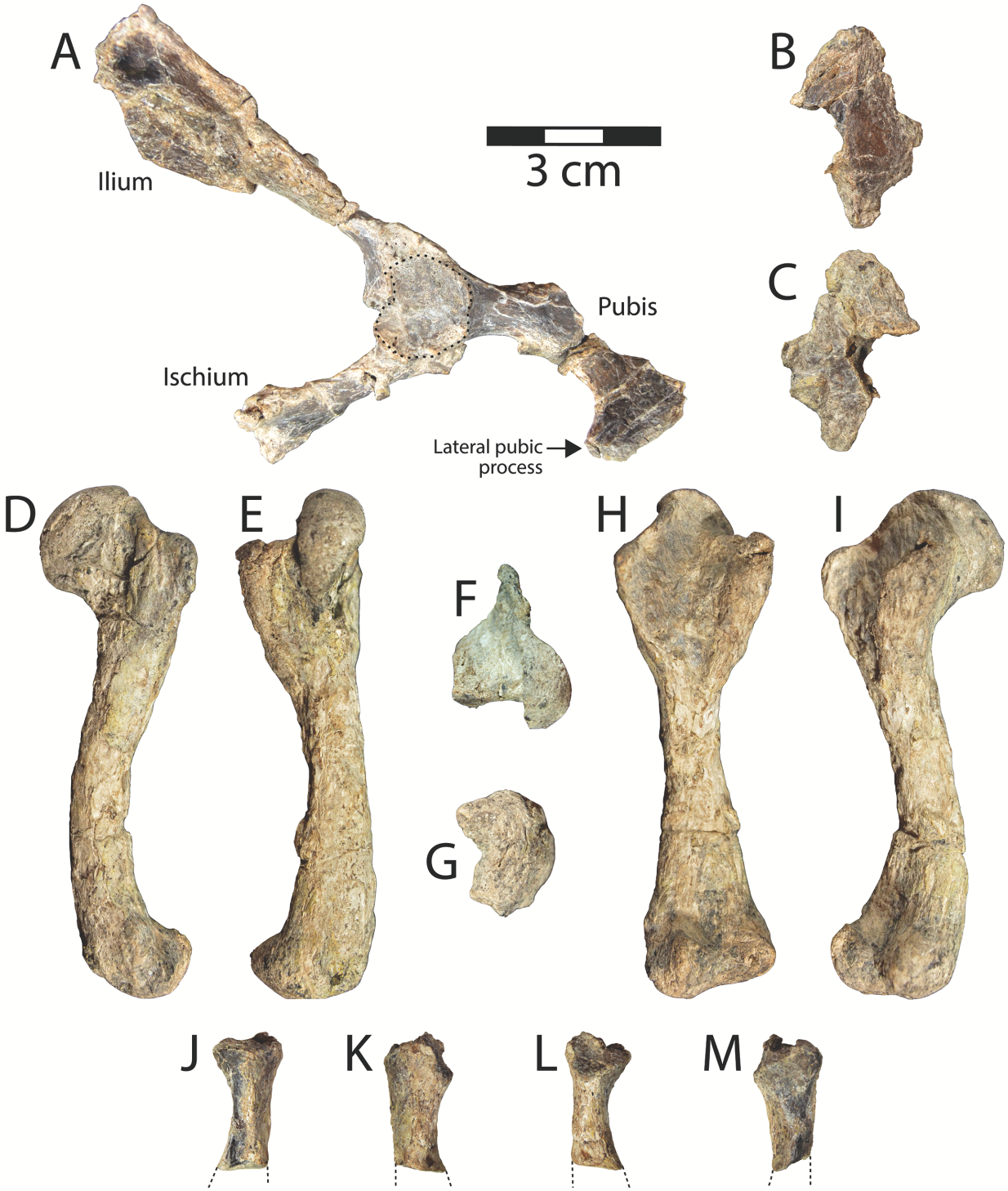

FIGURE 7. DMNH 2013-07-1942 pelvic girdle and hind limb bones. Partial pelvis in A, right lateral view, oriented with anterior to the right. Partial pubic plate in B, ventral, and C, dorsal views. Left femur in D, anterior, E, ventral, F, proximal, G, distal, H, dorsal, and I, posterior views. Partial right tibia in J, dorsal, K, medial, L, ventral, and M, lateral views. Dotted line in G indicates margin of acetabulum.

ance and not part of the acetabulum concavity (Figure 7A). The acetabulum measures 16.6 mm dorsoventrally and 17.5 mm anteroposteriorly. The maximum mediolateral thickness of the acetabulum complex is 14.2 mm. The ischial contribution to the acetabulum is broken and twisted medially so that it is slightly displaced and discontinuous with the ilium (Figure 7A). Thus, the preserved ischial neck and triangular ischial blade have been somewhat turned from their natural mediolateral orientation. The ischial neck measures 11.6 mm wide and 5.9 mm thick, and it projects posteroventrally from the acetabulum. The flattened blade-like portion of the ischium is 22.7 mm wide, 5.3 mm thick distolaterally, and 2.4 mm distomedially (Figure 7A). The ilium is broken through its neck, which projects posterodorsally from the acetabulum (Figure 7A). The iliac neck is 11.7 mm wide and 4.5 mm thick at its broken edge. The separate iliac blade is 48.2 mm long and 41.5 mm wide, and was probably oriented more mediolaterally in anatomical position (Figure 7A). The blade itself is shallowly concave in the middle from apparent crushing, and its distomedial corner is missing (Figure 7A). The bone has a maximum thickness of 3 mm along its distal margin. The neck of the pubis is intact, 8.7 mm thick, and projects anteroventrally from the acetabulum.

The lateral pubic process is approximately 12 mm wide at the base, 10.1 mm long, and reaches a maximum thickness of 3.6 mm (Figure 7A). On the medial side of the separate pubic fragment there is at least part of a smooth, unsutured, concave articular facet, likely representing a movable articulation with the plastron, which is present in generalized cryptodires such as baenids and pleurosternids (Gaffney, 1990). This constitutes the only apparent articulation between the pelvis and shell in DMNH 2013-07-1942. A final, isolated fragment found near the pelvis is interpreted as part of the pubic plate, measuring 35.1 mm long and 23.6 mm wide, and missing most of its posterior right portion (Figure 7B-C). The fragment is anteriorly curved, convex ventrally, and reaches 7.7 mm thick at the midline (Figure 7B-C). Possible articular edges are indistinguishable, it has a ventral ridge along the midline, and its dorsal surface is irregularly rugose.

Due to the fragmentary and distorted nature of the pelvis in DMNH 2013-07-1942, detailed comparisons with other published baenid pelves are not possible. However, the pelvis of *Gehennachelys maini* comb. nov. can be said to be generally consistent with known baenid pelves (e.g., *Neurankylus hutchisoni* [Hutchison et al., 2013] in Lively 2016, figure 3; *Neurankylus baueri* and *N. torrejonensis* in Lichtig and Lucas 2018, figures 17, 21A-B, 22f-g, 31D-E; *"Baena" affinis* Leidy 1871b [*Baena sima* of Hay, 1908] and *Chisternon undatum* in Hay 1908, figures 54, 85-86; *Plesiobaena antiqua* in Brinkman 2003, figure 7C; and *Eubaena cephalica* in Archibald 1977, figure 85).

The left femur is complete, 85.1 mm in total length, and though its surface is somewhat degraded, most important morphologies are preserved (Figure 7D-I). The femur is generally similar to other turtles, with a distinct, ventrally-inclined head that reaches 21.4 mm long and 10.4 mm wide (Figure 7E). The greatest width of the proximal femur is 31.9 mm (Figure 7F). The articular surface of the femoral head is elliptical and elongate (Figure 7E). It projects proximoventrally from the femoral shaft at an angle of approximately 120° (Figure 7D, I). In posterior view, the articular surface of the femoral head is curved, but its length is still more than twice the width (Figure 7A). The major and minor trochanters are distinct but connected to the femoral head, and the minor trochanter is the more robust (Figure 7E-F, H). The minor trochanter projects approximately perpendicular to the femoral neck and is thick and blocky (Figure 7F). In comparison, the major trochanter is thin and bladelike. A slightly thickened ridge runs along the proximal and ventral margin of the major trochanter, and is continuous with the proximal end of the femoral head (Figure 7F). When viewed proximally, the trochanters project at approximately 90° from each other. Viewed ventrally, the femoral head is significantly taller than either trochanter, and the minor is slightly taller than the major (Figure 7H). The intertrochanteric fossa is deep and well defined. It is open dorsally and proximally, and is longer than wide (Figure 7H). The femoral shaft is arched ventrally and has a diameter of 10.2 mm at midshaft (Figure 7D-I). As in other turtles, the distal end of the femur consists of two condyles that are separated by a V-shaped depression, the posterior of which is larger. The greatest width of the distal femur is 23.5 mm (Figure 7G). Viewed distally, the condyles form a nearly continuous articular surface (Figure 7G-H). There is a small, but distinct fibular epicondyle that projects anteriorly from the anterior condyle (Figure 7D-G).

The femur of *Gehennachelys maini* comb. nov. is similar to that of other known baenids, though not many examples are available for comparison. Compared with *"Baena" affinis* Leidy, 1871b (*Baena riparia* of Hay, 1908), the femur of *G. maini* comb. nov. has a longer neck with a head

that is tilted posteriorly, and a wider minor trochanter (Hay 1908, figures 65, 66a). Compared to *Neurankylus torrejonensis,* the femoral head of *G. maini* comb. nov. has a slightly longer neck, and is more proximally oriented (Lyson et al. 2016, figure 5.3; Lichtig and Lucas 2018, figures 15J-O, 31F-G). The intertrochanteric fossa is also longer, and the femoral shaft more curved in *G. maini* comb. nov. The development of the fibular epicondyle is consistent in the two taxa. Similarly, *Neurankylus baueri* has a straighter femoral shaft, shorter intertrochanteric fossa, less prominent trochanters, and a less projecting, proportionally wider femoral head than *G. maini* comb. nov. (Lichtig and Lucas 2018, figures 21C-F, 22a-b). The femoral head of *G. maini* is more proximally oriented with a longer femoral neck than *Eubaena cephalica*, and its femoral shaft is more curved (Archibald 1977, figure 84a). The femur of *G. maini* comb. nov. is quite similar to that of *Thescelus insiliens* Hay, 1908 (*Baena longicauda* of Russell, 1934), except the major trochanter projects slightly more proximally in the former (Russell 1934, plate 3, figure 3-4). The femoral head of *Plesiobaena antiqua* (*Baena antiqua* of Russell, 1934) is proportionally wider and projects further dorsally than in *G. maini* comb. nov., but otherwise the two taxa are similar (Russell 1934, plate 5, figure 4-5). Compared with *Glyptops plicatulus* of Hay, 1908, the humerus of *G. maini* comb. nov. is very similar, but has a slightly wider proximal expansion and a slightly taller minor trochanter (Hay 1908, figures 25-26).

A single partial proximal tibia is preserved from DMNH 2013-07-1942, measuring 23.1 mm long, and with a maximum proximal width of 12.7 mm and maximum distal width of 10.0 mm (Figure 7J-M). The morphology of the tibia in turtles varies primarily by length and proximal width (Gaffney, 1990). As such, total proportions cannot be determined for DMNH 2013-07-1942, nor can the morphology of the distal tibia. The proximal tibia is consistent with the condition described in Gaffney (1990) where a shallow, posteromedial concavity articulates with the medial femoral condyle, and a flatter facet corresponds with the trough between femoral condyles (Figure 7J-M). The proximal tibia of *Neurankylus lithographicus* Larson, Longrich, Evans, and Ryan, 2013, provides the only point of comparison among baenids, and is similar in morphology to *Gehennachelys maini* comb. nov., but the shaft of the former is straighter (Lichtig and Lucas 2018, figure 27A-C).

Shell Reconstruction of *Gehennachelys maini* comb. nov.

Through the description and addition to the hypodigm of additional shell, cranial, and postcranial material, a more comprehensive morphological understanding of *Gehennachelys maini* comb. nov. has been realized. Using the complete shell of HMNS-10-TM, overall shape, dimensions, and proportions of an apparently fully adult individual were determined, providing the overall framework for a reconstruction of the shell (Figure 8; see Appendix 1 for measurements of relevant specimens). Fortunately, a single specimen (DMNH 2013-07-0784) preserved sulci on most of the carapace (Adrian et al. 2019, figure 2.1-2, 2.4-7). The size of the carapace of DMNH 2013-07-0784 is estimated to be approximately 27 cm (Appendix 1), which suggests a subadult individual when compared to the carapace length of approximately 39 cm in HMNS-10-TM, the only known complete and articulated shell (Figure 4; Appendix 1). Plastral and bridge sulci were reconstructed from figured specimens in the original description of *"Trinitichelys" maini* (Adrian et al., 2019): the holotype DMNH 2013-07-0712 (figure 3.1-4), DMNH 2013-07-0704 (figure 3.5-8), DMNH 2013-07-0696 (figure 3.5-8), DMNH 2013-07-1703 (figure 3.13-17), and DMNH 2013-07-1708 (figure 3.18-21). The reconstruction depicts an anal notch, which is variably present in *G. maini* comb. nov. and modeled after DMNH 2013-07-1942. Another polymorphic trait, the nuchal notch, is depicted in the reconstruction after the only known specimen of *G. maini* comb. nov. showing the trait—DMNH 2013-2013-07-0784 (Adrian et al., 2019: figure 2.1-2.2).

The reconstructed shell of *Gehennachelys maini* comb. nov., along with the measurements of a fully grown adult (HMNS-10-TM), provide insights into previously unknown morphological characters, some of which are phylogenetically relevant (Figure 8; Table 2). Further, comparisons can be made with other baenid taxa for which associated carapaces and plastra are known (Figure 9). In Figure 9, the ratio of plastron length to carapace length is plotted against that of anterior plastral lobe length to posterior plastral lobe length (raw data in Table 3). Patterns within the resulting plot of relative proportions suggests a weak underlying phylogenetic structure (Figure 9). The graph retrieves *Gehennachelys maini* comb. nov. as being one of two taxa (the other being *Thescelus insiliens*) with plastra and carapaces of approximately equal length, and *Saxochelys gilberti* Lyson, Sayler, and Joyce, 2019, as the only sam-

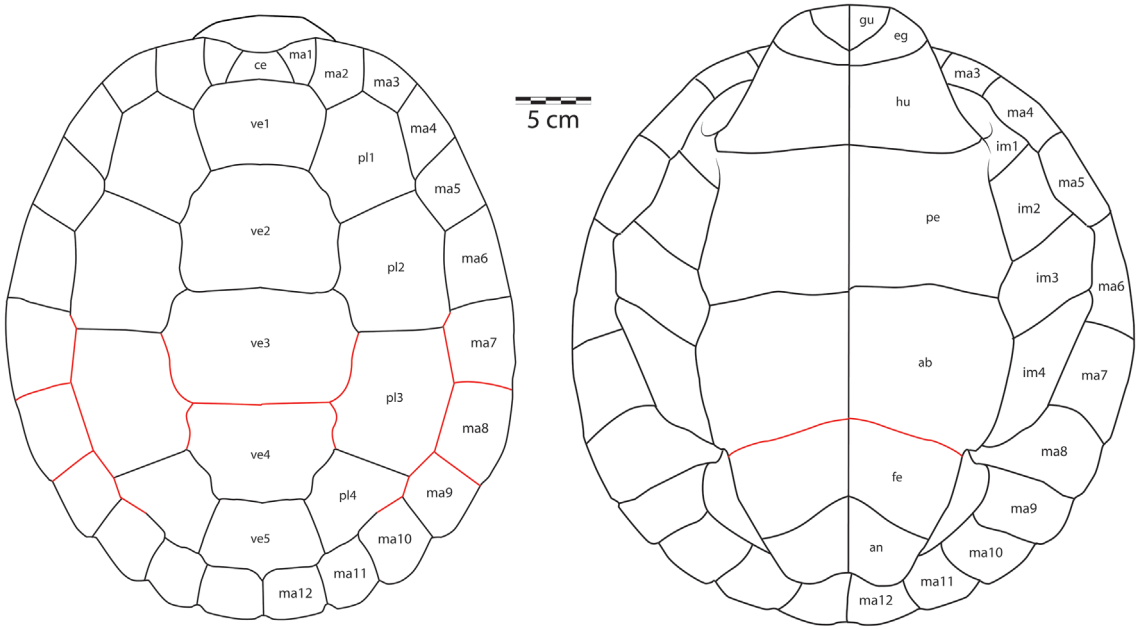

FIGURE 8. *Gehennachelys maini* comb. nov. shell reconstruction, based on DMNH 2013-07-0696, DMNH 2013-07-0704, DMNH 2013-07-0712, DMNH 2013-07-0784, DMNH 2013-07-1703, DMNH 2013-07-1708, DMNH 2013-07-1942, and HMNS-10-TM. Red lines indicate estimated sulci. Abbreviations: ab= abdominal scale, an= anal scale, ce= cervical scale, eg= extragular scale, fe= femoral scale, gu= gular scale, hu= humeral scale, im= inframarginal scale; ma= marginal scale, pec= pectoral scale, pl= pleural scale, ve= vertebral scale.

TABLE 2. Comparison of traits from basal baenids and basal baenodds with known skulls, carapaces, and plastra. Data obtained from: Gilmore, 1920; Brinkman, 2003; Lyson and Joyce, 2009a; Joyce and Lyson, 2015; Lively, 2015; Joyce et al., 2020; Rollot et al., 2022a, b.

Trait	***Lakotemys australodakotensis***	***Trinitichelys hiatti***	***Gehennachelys maini* comb. nov.**	***Arvinachelys goldeni***
Age	Berriasian–Valanginian	Aptian–Albian	Cenomanian	Campanian
Parietal-squamosal contact	Present	Present	Absent	Absent
Nasals	Slightly reduced	Reduced	Reduced or absent	Enlarged
Squamosal processes	Not elongated	Elongated	Elongated	Not elongated
Upper temporal emargination: visibility in dorsal view of anterior portion of otic capsule	Not visible	Not visible	Visible	Visible
Crista supraoccipitalis: anterior coverage by parietals	Halfway	Extensive	Minimal	Extensive
Jugal contribution to posterior orbital margin	Absent	Absent	Present	Present
Relative size of frontals and parietals	Parietals larger	Parietals larger	Parietals larger	Frontals larger
Midline extragular contact	Absent	Absent	Present, relatively short	Gular scales absent
Larger plastral lobe	Anterior	Posterior	Equidimensional	Posterior
Plastral length (cm)	~28	~29	36.3	29.1
Vertebral scale 1 narrowing	?	Posteriorly	Posteriorly	Posteriorly
Vertebral scale 3 dimensions	Equidimensional	Wider than long	Wider than long	Wider than long
Femoral-anal sulcus shaped	Straight	?	Straight	Omega-shaped
Vertebral scale contribution to posterior margin	Probably absent	Probably absent	Absent	Present

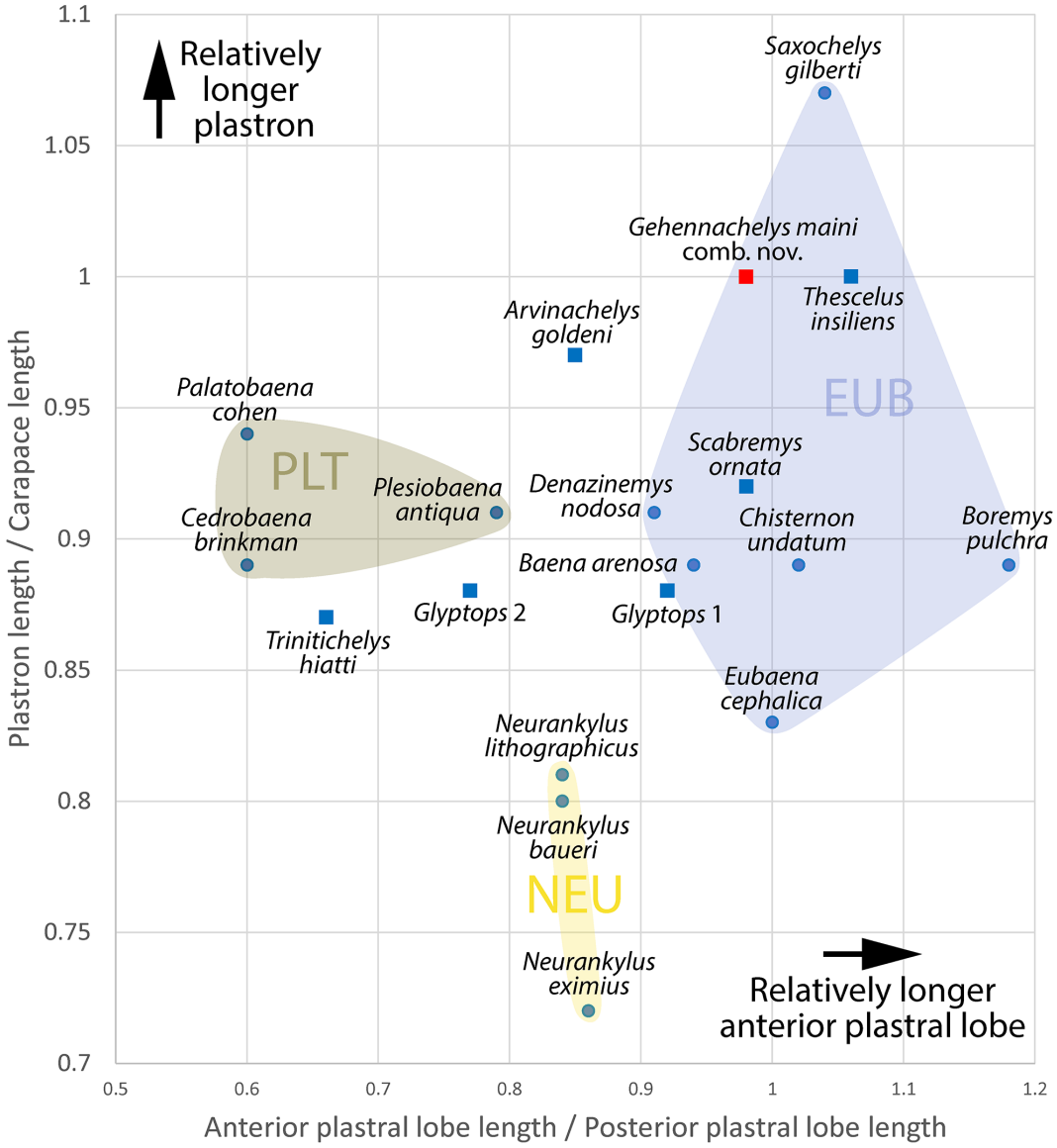

FIGURE 9. Plot of Plastron Length/Carapace Length by Anterior Plastral Lobe Length/Posterior Plastral Lobe Length for baenid taxa and *Glyptops*, which have associated carapaces and plastra. Proportions of *Gehennachelys maini* comb. nov. from HMNS-10-TM. Data on other taxa from Archibald (1977, table 57), Lyson and Joyce (2009a, b), Larson et al. (2013), Sullivan et al. (2013), Lively (2015), and Lyson et al. (2019). See Table 3 for raw data. Graph generated in Microsoft Excel. Grouping abbreviations: EUB= Eubaeninae; NEU= *Neurankylus* spp.; PLT= Palatobaeninae/ *Plesiobaena* grade. Squares indicate phylogenetically ungrouped taxa (non-baenodd baenids and *Glyptops*), circles indicate phylogenetically grouped taxa (*Neurankylus* and baenodds), and red square indicates *Gehennachelys maini* comb. nov.

pled baenid with a longer plastron than carapace (Figure 9). *Gehennachelys maini* comb. nov. has a relatively longer plastron than 89.5% of sampled taxa (Figure 9). Most of the sampled taxa (which include basal baenodds and two representatives of *Glyptops* sp.) have plastral lengths in the range of 80–95% the lengths of the corresponding carapaces (Figure 9). Notably, the ratio of plastral to carapace length was lower in the three *Neurankylus* spp. than in the remainder of the sample, and the positions of *G. maini* comb. nov. and *T. hiatti* are quite different (Figure 9). The shells of *Trinitichelys hiatti* and *Glyptops* sp. were also low in relative plastral length among the sampled baenids (Figure 9). *Gehennachelys maini* comb. nov. has a relatively longer anterior plastral lobe compared to

TABLE 3. Relative proportions of complete baenid taxa, plus *Glyptops*. * indicates estimation of nearly-complete shell. Data from: Archibald (1977, table 53); Lyson and Joyce (2009b, figure 6); Larson et al. (2013, figure 21.5); Joyce and Lyson (2015: figure 2A); Lively (2015, figures 5C, 6C); Lyson et al., (2016, figure 4); Lyson et al., (2019, figure 6).

Taxon	Anterior lobe length / Posterior lobe length	Plastron length / Carapace length
Glyptops 1	0.92	0.88
Glyptops 2	0.77	0.88
Trinitichelys hiatti	0.66	0.87
Neurankylus eximius	0.86	0.72
Thescelus insiliens	1.06	1.00
Plesiobaena antiqua	0.79	0.91
Boremys pulchra	1.18	0.89
Scabremys ornata	0.98	0.92
Denazinemys nodosa	0.91	0.91
Eubaena cephalica	1.00	0.83
Baena arenosa	0.94	0.89
Chisternon undatum	1.02	0.89
Gehennachelys maini comb. nov.	0.98	1.00
Saxochelys gilberti	1.04	1.07
Arvinachelys goldeni	0.85	0.97
Palatobaena cohen	0.60	0.94
Neurankylus lithographicus	0.84	0.81
*Cedrobaena brinkman**	0.60	0.89
Neurankylus baeuri	0.84	0.80

the posterior than 68.4% of sampled taxa (Figure 9). The only taxa with relatively equal or longer anterior lobes are derived baenid forms (in ascending order): *Scabremys ornata, Eubaena cephalica, Chisternon undatum, Saxochelys gilberti, Thescelus insiliens,* and *Boremys pulchra* (Figure 9).

There is no clear trend between relatively longer anterior plastral lobes and degree of derivation, though *Gehennachelys maini* comb. nov. more closely groups with baenodds than with stem baenids or *Glyptops* specimens AMNH FARB 336 and AMNH FARB 1018 (Archibald, 1977) (Figure 9). In addition to being similar to aquatic taxa by its moderately domed, hydrodynamic shell forming a teardrop shape in lateral view, the baenid shell is notable for its relatively large plastron that covers much of the shell from below (Joyce and Lyson, 2015). The relative size of the plastral lobes produces distinct groupings with no overlap along the x-axis: a Palatobaeninae/*Plesiobaena* cluster with an anterior plastral lobe that is 60–79% the length of the posterior lobe, a *Neurankylus* spp. cluster near 84–86% in proportion, and a Eubaeninae cluster with a 91–118% proportion (Figure 9). Within this framework, *G. maini* comb. nov. groups with the Eubaeninae, though it is not phylogenetically retrieved within that clade (Figures 9, 11). The results of this analysis show a distinct phylogenetic signal but are currently inadequate to form the basis of ecological or functional inferences, especially since baenids have fundamental structural differences from cryptodires (i.e., constraints related to limited head retraction and the presence of fully formed mesoplastra) (Pritchard, 1966).

Paleohistology of *Gehennachelys Maini* comb. nov.

Two thin sections of costals were prepared from shell fragments of *Gehennachelys maini* comb. nov. recovered at the Arlington Archosaur Site (AAS) (Figure 10A-B). The size of the larger section (DMNH 2013-07-0588) is consistent with known adult specimens of *G. maini* comb. nov., and the smaller section (DMNH 2013-07-1703) comes from a significantly smaller individual (Figure 10A-B). The larger sample was taken from a costal fragment, with sulci suggesting identification as the fourth. The sides of the sample have preserved intercostal sutures, indicating the section was longitudinal (Figure 10B). The slight bulge in the middle of the internal surface represents a rib bulge, and the subtle nature of the curve suggests a rela-

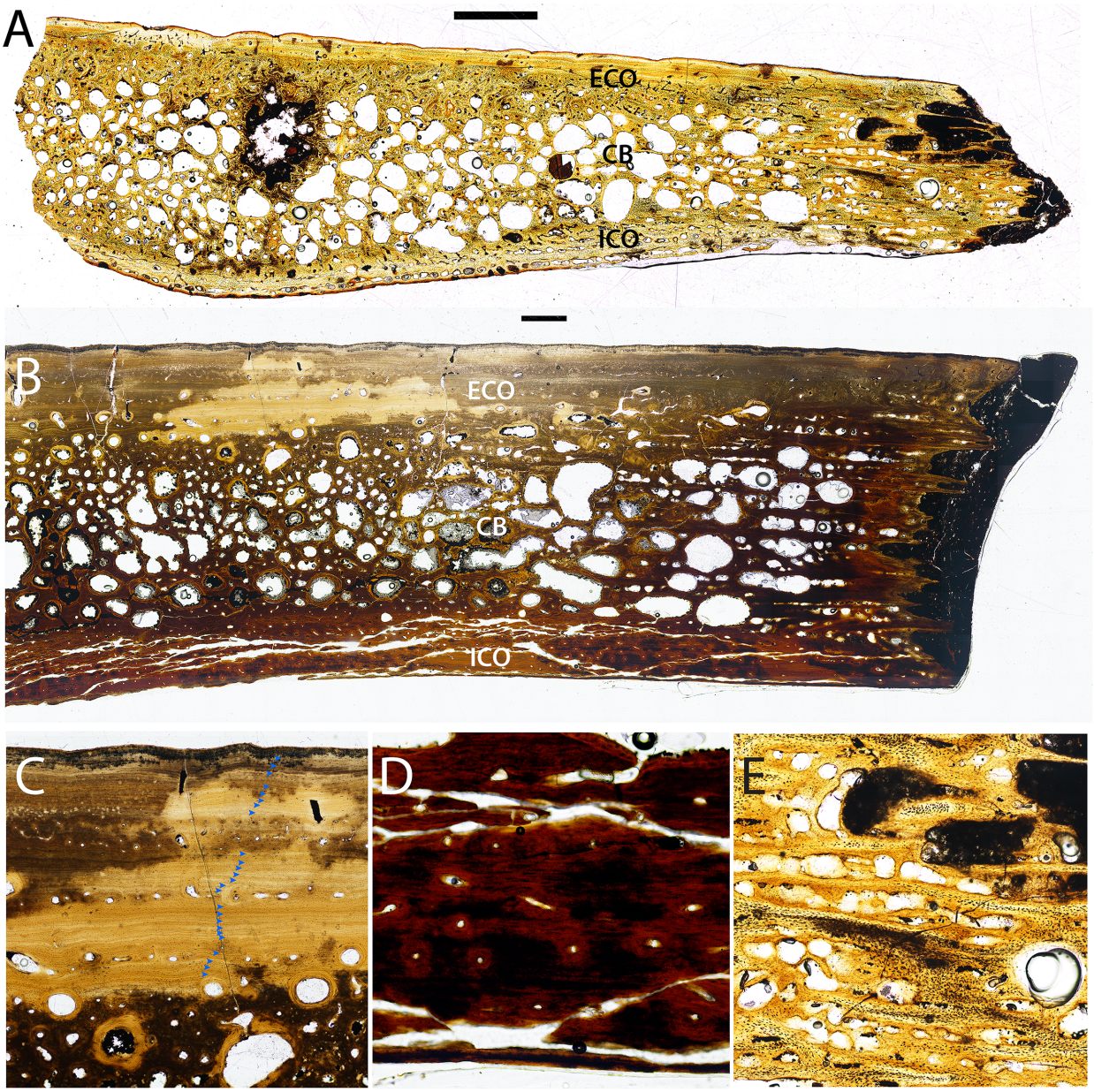

FIGURE 10. *Gehennachelys maini* comb. nov. histological thin sections: A, DMNH 2013-07-1703, an indeterminate juvenile costal, and B, DMNH 2013-07-0588, a probably fourth costal. Scale bars equal 1 mm. C, closeup of vascularized external cortex and transition to cancellous bone, with growth marks indicated by blue arrowheads, D, internal cortex with intercalated vascular rows from DMNH 2013-07-0588, and E, sutural sockets of DMNH 2013-07-1703. Abbreviations: CB= cancellous bone, ECO= external cortex, ICO= internal cortex.

tively lateral position of the section along the costal (Figure 10B). Most of the internal cortex of DMNH 2013-07-0588 is fractured by long, thin, sometimes convergent cracks, which are probably an artefact of histological slide preparation (Figure 10B, D). Several thin cracks also traverse the external cortex (Figure 10B). Due to damage to the thin section of DMNH 2013-07-0588, only half of the costal is described and figured in cross section (Figure 10B).

The juvenile costal represented by DMNH 2013-07-1703 was also longitudinally sampled, and includes half of the anteroposterior length with a preserved suture, and a rib bulge (Figure 10A). The thin section of DMNH 2013-07-1703 is well preserved, with the only notable damage to the internal cortex toward the sutured end, as well as

an elliptical hole in the interior cancellous bone near the middle of the rib bulge (Figure 10A). This hole is partially infilled with dark matrix, and probably resulted from taphonomic damage to the broken end of the sampled costal.

The thin section samples of *Gehennachelys maini* comb. nov. are similar to previously described baenid paleohistology, and have a diploë structure typical for turtles, with internal and external compact layers enclosing interior cancellous bone (Scheyer, 2007) (Figure 10A-B). The external and internal cortices of *G. maini* comb. nov. have variable thickness. Measured from DMNH 2013-07-0588, the external cortex is 114% thicker than the internal, however, in DMNH 2013-07-1703, the external cortex is 71% of the internal thickness (Figure 10A-B). Few full-thickness images of baenid shell histology have been published, but the cortices of *Neurankylus baueri* are approximately equal in thickness, as in *G. maini* comb. nov. (Lichtig and Lucas, 2018). In contrast, the exterior cortex of *Denazinemys nodosa* Gilmore, 1916, is far thicker than the interior cortex, at least in part because of prominent, raised pustules that ornament the exterior carapace (Lichtig and Lucas, 2017). The external cortex of *G. maini* comb. nov. consists of interwoven structural collagenous fiber bundles (ISF) (Scheyer, 2007). The external cortex is composed of generally thinner external and thicker internal portions (Figure 10B-C). The external portion is formed by parallel fibered bone, and the interior portion is comprised of fiber bundles that extend perpendicular, sub-parallel, and diagonally to the external surface of the bone (Figure 10C). In the exteriormost perpendicularly fibered portion of the external cortex of DMNH 2013-07-0588, there are a few parallel rows of small, irregularly spaced, mostly elliptical or round primary vascular canals and primary osteons, intercalated with avascular parallel layers, indicating low vascularization as in *Plesiobaena antiqua* and *Neurankylus* sp. (Scheyer, 2007) (Figure 10C). As in other sampled baenids, vascularization increases toward the interior cancellous bone (Scheyer, 2007) (Figure 10B-C). The parallel fibered layers of the exteriormost region are wavy near its transition with more interior bone (Figure 8B). In this layer, there are distinctive, laterally traceable growth marks in both individuals sampled. In DMNH 2013-07-0588, there are at least 25 distinct growth marks, and in DMNH 2013-07-1703, there are at least ten.

The interior cancellous bone of *Gehennachelys maini* comb. nov. consists of predominantly short, thick, irregular trabeculae and small vascular spaces (Figure 10A-B). Trabeculae vary significantly in size, and most are subcircular, elliptical or appear as coalesced ellipses (Figure 10A-B). The maximum size of the trabeculae appears to scale with the rest of the bone, reaching approximately 0.75 mm in DMNH 2013-07-1703, and 1.68 mm in DMNH 2013-07-0588. As in other baenids, vascularization of the cancellous bone is represented by large secondary osteons and erosion cavities (Scheyer, 2007). Vascular cavities and trabeculae in the cancellous bone are largest in the interiormost portion (Figure 10A-B). Trabecular walls consist of lamellar bone, containing bone cell lacunae that are mostly flattened, elongated, and aligned with the lamellar layers. Primary bone tissue consisting of ISF is mostly still present at the centers of trabeculae and in branching areas. Unlike the external cortex and the internal cortex of *Neurankylus* sp., the cancellous bone of *G. maini* comb. nov. transitions abruptly into the parallel-fibered bone of the internal cortex (Scheyer, 2007) (Figure 10A-B). The internal cortex of *G. maini* comb. nov. is thinner than the external, and its vascularization is low to moderate, as typical in baenids (Scheyer, 2007) (Figure 10A-B, D). A few strongly vascularized layers consist of small, round or elliptical, regularly spaced primary osteons or primary vascular canals, similar to *Plesiobaena antiqua* (e.g., Scheyer 2007, figure 37g). As in the external cortex, the vascularized layers are intercalated with avascular layers of parallel-fibered bone (Figure 10D). As in other baenids, the sutures consist of bony protrusions and sockets (Scheyer, 2007) (Figure 10A-B, E). In the larger DMNH 2013-07-0588, black matrix filled the sockets of the suture and infiltrated some vascular and erosional cavities (Figure 10B). The protrusions in the sutures are irregular in size and arrangement, and some are filled with a single row of cavities that transitions into the network of larger cavities in the cancellous bone (Figure 10E). The paleohistology of *G. maini* comb. nov. is broadly similar to that of known baenids and the pleurosternid *Glyptops plicatulus* Cope, 1877, however the internal cortex of the latter is avascular except for near rib bulges in costals (Scheyer, 2007).

Phylogenetic Placement of *Gehennachelys maini* comb. nov.

Coding of *Gehennachelys maini* comb. nov. is provided in Appendix 2, and the full data matrix is available as Supplementary Data. The phylogenetic analysis resulted in 170 most parsimonious trees of 367 steps (Figure 11). No taxa were identi-

FIGURE 11. Results of phylogenetic analyses for *Gehennachelys maini* comb. nov., produced from the modified matrix Rollot et al. (2022b), with 170 minimum trees and 367 steps (CI= 0.35; RI= 0.71): A) Consensus 50% majority-rule phylogenetic tree of Baenidae; B) Strict consensus tree. Yellow stars indicate *Gehennachelys maini* comb. nov.

fied as "rogue" by the pruned trees function, and thus all original taxa were retained in the analysis. In the 50% majority rule consensus tree, *Gehennachelys maini* comb. nov. fell in a large, unresolved polytomy at the base of Baenodda with six other baenid species (Figure 11A). The newly combined taxon was positioned quite distantly from *Trinitichelys hiatti*, which fell as a basal baenid outside the clade of *Neurankylus* + Baenodda (Figure 11A), consistent with recent re-analyses of the

phylogenetic position of *T. hiatti* (Rollot et al., 2022b). In the strict consensus tree, *G. maini* comb. nov. was positioned in a large, unresolved polytomy at the base of Baenodda with 17 other baenid species (Figure 11B).

DISCUSSION

Character Optimization and Morphology of *Gehennachelys maini* comb. nov. in Relation to Baenodda

As with many baenid species, *Gehennachelys maini* comb. nov. is defined by a unique combination of characters, rather than multiple autapomorphies. Its phylogenetic position at the base of the clade of Baenodda (Figure 11) reflects its unique combination of primitive and derived states. It shares certain characters with Baenodda (especially in the skull), while still retaining some of the primitive characters found in early baenids such as *Trinitichelys hiatti* and *Lakotemys australodakotensis* (Gaffney, 1972; Joyce et al., 2020) (Table 2).

Character optimization revealed that the base of Baenodda is defined by eight common, unambiguous synapomorphies: frontal-maxilla contact (character 16:1), loss of parietal-squamosal contact (character 20:1), tubercle on posterolateral edge of dentary (character 30:1), gular scales that are smaller than the extragulars (character 46:0), medial contact of the extragulars (character 47:1), z-shaped xiphiplastron-hypoplastron suture (character 49:1), pygal notch (character 50:1), and contribution of the fifth vertebral scale (Ve5) to the posterior margin of the carapace (character 33:1), although the final character was reversed in *Gehennachelys maini* comb. nov. Compared to other baenodd clade, *Gehennachelys maini* comb. nov. is unique in having frontals that do not extend posteriorly beyond the orbit (character 14:1), vertebral scales that are generally wider than long (character 39:0), anterior margin of marginal 1 mostly over the nuchal (character 44:0) V-shaped anterior peripherals (character 103:1), and the aforementioned lack of Ve5 contribution to the posterior carapacial margin (character 33:0).

In the cranium, *Gehennachelys maini* comb. nov. also shares with other baenodds characters that are not captured in the phylogenetic analysis such as deep temporal emargination in which the anterior margin of the otic capsule is visible in dorsal view and reduced nasals (except in *Arvinachelys*) (Table 2). In contrast, it shares with at least some early baenids, such as *Trinitichelys hiatti* and *Lakotemys australodakotensis,* extensive squamosal processes. This trait could be either homoplastic or a symplesiomorphic retention.

Gehennachelys maini comb. nov. is most unique in the composition of its posterior cranial crests. In particular, the crista supraoccipitalis is more prominent and exposed with reduced parietal coverage anteriorly than other baenids. The tips of the squamosals are also lengthy, pointed, and appear slightly curved (Table 2; Figure 2). In the shell, *Gehennachelys maini* comb. nov. shares a midline extragular contact (character 47:1) and a posteriorly narrowing vertebral scale 1 with baenodds, but it differs in having a straight femoral-anal sulcus and lacking vertebral scale contact with the posterior carapace margin (character 33:0) (Table 2). While several of these traits were not captured by the phylogenetic analysis, the combination of characters is consistent with the interpretation of *G. maini* comb. nov. as possessing both symplesiomorphic and derived baenodd features. This is perhaps unsurprising given its status as the earliest of the species recovered within Baenodda (Figure 11).

Historically, Baenodda was defined by presence of a fifth vertebral scale that contacted the posterior margin of the carapace (e.g., Gaffney and Meylan, 1988 and Joyce and Lyson, 2015). Our character optimization revealed that this character state change occurred at the base of Baenodda and characterizes all other baenodds except *Gehennachelys maini* comb. nov. However, as more basal members of the derived baenid clade are recognized, the mosaic nature of character evolution in non-basal baenids is further revealed. It is now clear that the baenodd clade cannot be exclusively defined by the aforementioned character state. Other taxa that fall in the lineage leading to Baenodda without having the full suite of derived characters include *Thescelus* spp., which have omega-shaped femoral-anal sulci and complete marginal rings, and *Scabremys ornata* and *Eubaena hatcheri* (*"Baena" hatcheri* of Hay, 1901), which have the reversed condition for both traits (Hay, 1908; Sullivan et al. 2013; Lyson et al., 2019). It is intriguing that the posterior shell seems to be the location of the last morphological steps of baenid taxa toward the derived state (Table 2).

Taphonomy

The remains of *Gehennachelys maini* comb. nov. referred in the current study are from two closely-located sites in the Lewisville Formation of the Woodbine Group (Figure 1B). The localities occur in deposits with similar composition, and are

also like the nearby *Protohadros byrdi* type locality at Flower Mound (Head, 1998; Noto, 2015). However, the two most complete known shells of *G. maini* comb. nov. have quite different states of preservation (Figures 3-4). The shell of DMNH 2013-07-1942 was discovered badly crushed and right side up, with the entire shell broken into pieces mostly smaller than approximately 8 cm^2 (Figure 3). The bridges are collapsed, the plastron was shifted to the left, and transport of shell fragments was minimal enough that the entire specimen was excavated in one jacket (Noto 2015, figure 10C) (Figure 3). All of the associated postcranial elements were similarly transported a minimal distance, with many displaced, though near their original anatomical position (Figures 5-7). In particular, some right forelimb material was preserved below the skull, with the probable acromial process of the right scapula attached to the ventral side of the skull (Figure 2C-D). Elements as small as cervical vertebrae are distorted and have numerous missing processes (Figure 5A-C). This is consistent with the general pattern of deposition of vertebrate remains from Facies A of the Arlington Archosaur Site (AAS), where fossils are well preserved, but almost entirely disarticulated, with some elements contorted out of anatomical position and separated by 2–3 m (Noto, 2015). The particular deposition of DMNH 2013-07-1942, which preserves most of the individual, indicates that deposition likely occurred less than 20 weeks postmortem, which is the time by which heads with necks and appendages typically disarticulate in modern aquatic turtles (Brand et al., 2003).

A parautochthonous origin is indicated for fossils from the AAS by lack of evidence for long-distance aqueous transport or prolonged subaerial weathering features (Noto, 2015). The widespread disarticulation of remains in Facies A is interpreted to be a result of tidally forced water level fluctuations which caused short distance displacement (Noto, 2015). Over time, disarticulation and spreading of the remains occurred without transport induced damage (Noto, 2015). Bones from Facies A show no apparent horizontal orientation preference and occur at various vertical angles, probably from shrink-swell cycles and or bioturbation (Noto, et al. 2012). A survey of more than 200 such bones showed most fall within weathering stages 0 or 1, with little evidence of sediment abrasion due to aqueous transport (Behrensmeyer, 1978; Noto et al., 2012). Many broken fossils exhibit transverse fracturing consistent with breakage after fossilization (Fiorillo et al., 2000; Noto et al., 2012).

The preservation and deposition in HMNS-10-TM from the Grapevine Lake shoreline is quite different than DMNH 2013-07-1942 (Figure 4). First, HMNS-10-TM had no associated cranial or postcranial material, indicating that the head and appendages had probably become separated due to decomposition and/or scavenging before the shell was buried. Considering the known rates of disarticulation among modern aquatic turtles, this probably occurred more than 20 weeks postmortem (Brand et al., 2003). The shell is entirely infilled with hard, iron-cemented sandstone, which supported the interior of the shell and prevented its flattening (Figure 4C-E). The iron-cemented sandstone infilling the shell occurs in at least thin layers along the Grapevine Lake southwest shoreline, but not the AAS, and it can contain invertebrate traces and borings (Figure 1B). It is noteworthy that HMNS-10-TM was not preserved in the pervasive gray marine mudstone or overlying sandy layer at the locality. The ironstone infilling of the shell was likely formed by an active combination of meteoric waters and bacterial activities involving an ancient inundation of freshwater, which suggests direct association of the specimen with a fluvial, rather than tidal, channel (Selley et al., 2005; Akinlotan, 2019).

Taken together, the deposition of HMNS-10-TM is consistent with fast deposition following disarticulation of the head, neck, and appendages in a sandy fluvial or levee setting, possibly after bloating and washing down a nearby fluvial or tidal channel. There is no evidence of crocodile tooth marks. Additional chemical processes affecting deposits at the AAS may have contributed to the degradation of some recovered fossil specimens. During late diagenesis, external oxidants (oxygen, nitrate, nitrite, ferric iron Fe^3, and others) can enter fossil bone and alter its mineral composition (Pfretzschner, 2004). Pyrite formed earlier in diagenesis can be later oxidized and transformed into hematite, producing sulphuric acid in the process (Pfretzschner, 2004). Adjacent bone matrix is then etched and apatite is secondarily replaced by iron oxides (Pfretzschner, 2004). Sulfur bands, gypsum, and pyrite are prevalent throughout the dark gray carbonaceous sandy siltstone that comprises the most fossiliferous layer in Facies A at the AAS, and some specimens are encrusted entirely with gypsum crystals (Noto, 2015). During preparation, AAS fossils soaked in water have dripped liquid that was observed to dissolve holes into underlying

aluminum foil. Considerable gypsum invasion of fossil specimens has also been observed from the Grapevine Lake Dam Spillway, and iron is visibly present in the sandstone infilling of the shell of HMNS-10-TM (Tykoski and Fiorillo, 2010). Though not fully understood, the presence of a sulfur rich environment suggests a diagenetic scenario which may have chemically degraded some Lewisville Formation fossils over time. Such diagenetic conditions may be at least partially responsible for subtle alteration such as surface degeneration of turtle shell bone, which could eliminate thin and shallow sulci. Siderite is known from the AAS, particularly in facies C, but also as concretions in facies B (Main et al., 2010; Noto, 2015). Also, siderite is present in the Tarrant Fm. of the Eagle Ford Gp., which has been placed by some authors (e.g., Stephenson, 1952; Clark, 1965) in the Lewisville Fm. of the Woodbine Gp. (Denne et al., 2016). Sideritic ironstones have been geochemically associated with a chemically pure freshwater origin, which suggests reducing or anoxic conditions (Akinlotan, 2019). Such association is consistent with the typical deposition of baenids in freshwater, sandstone channels (Holroyd and Hutchison, 2002).

CONCLUSIONS

A diverse array of theropod dinosaur taxa appears in Laramidia by the Cenomanian and demonstrates a major turnover of terrestrial faunas (Cifelli et al., 1999; Eaton et al., 1999; Zanno and Makovicky, 2013; Zanno et al., 2019). The distinct similarity between the theropod assemblages of the Lewisville Formation (Fm.) and western sites, particularly at the Cedar Mountain (Mussentuchit Member) and Naturita ("Dakota") Formations in Utah, suggests two equally plausible scenarios that are not mutually exclusive. First, the similarity might be explained by the initial division of a cosmopolitan fauna during the distinct highstand event in the late Albian. The similarity could also be due to dispersal between Laramidia and Appalachia during the early Cenomanian regression (Noto et al., 2022).

Data from turtle components of the fauna bear on this question. The lack of a pleurosternid and presence of a baenid in the Lewisville Fm., and the reversed situation (with baenids absent, *contra* Avrahami et al., 2018) in the Cedar Mountain Fm. does not support a hypothesis of similarity due to previously shared cosmopolitanism. Also, the baenid taxa in north central Texas during the Late Albian *(Trinitichelys hiatti)* and middle Cenomanian (*Gehennachelys maini* comb. nov.) are distinctly different, with *G. maini* being significantly more derived. This also suggests that *G. maini* comb. nov. dispersed to north central Texas during the early Cenomanian (*Neogastroplites haasi* Reeside and Cobban, 1960 ammonite zone, 99–98.5 Ma), from surrounding land in Appalachia, or across the land bridge to Laramidia that extended through northern New Mexico and southern Colorado, by which time *Trinitichelys hiatti* was no longer present (see Blakey 2014, pages 21-25). A recent reevaluation of the skull of *T. hiatti* found it to be "nearly identical" to that of *Arundelemys dardeni* from eastern Appalachia, for which a shell is unknown (Rollot et al., 2022b). The current study demonstrates that the skull of *Gehennachelys maini* comb. nov. is considerably more derived than that of *T. hiatti* and *A. dardeni* and shares greater morphological affinity with Laramidian forms (Figure 11). While the ancestor of *Gehennachelys maini* gen. et sp. nov is unknown, it is more parsimonious to reconstruct the lineage as having a geographic origin in the west given the affinities between *G. maini* gen. et sp. nov and numerous later Laramidian forms.

Paleobiogeographic patterns from the late Albian to middle Cenomanian are complex and clade specific, but they indicate a gradual, rather than abrupt, ecological shift in dominant taxa (Adams et al., 2017; Adrian et al., 2019, 2021; Cavin et al., 2021; Noto et al., 2022). In the case of Lewisville Fm. turtles, remnants of a formerly cosmopolitan fauna and recent aquatic transcontinental immigrants were isolated by Cenomanian marine highstands and became integrated into a distinctive local fauna in southwest Appalachia. The taxonomic revision in the current study indicates a more derived phylogenetic position of the Lewisville Fm. baenid than previously understood. The replacement of the stem baenid *Trinitichelys hiatti* (Gaffney, 1972) by the derived *Gehennachelys maini* comb. nov., along with the appearance of trionychid and bothremydid immigrants (Adrian et al., 2019, 2021), and the disappearance of fully marine turtles in Texas such as the sandownid *Leyvachelys cipadi* Cadena, 2015, and possible toxochelyids (Thurmond, 1974), indicate a major turnover in the turtle assemblages of north central Texas between the Albian Trinity Group and the Cenomanian Lewisville Formation.

ACKNOWLEDGEMENTS

The authors would like to thank Dr. Ron Tykoski and Karen Morton at the Perot Museum of Nature and Science for access and logistical assis-

tance with specimens. Several workers from the Arlington Archosaur Site are recognized, including founder of the AAS project Derek Main and volunteers Art Sahlstein, Brad Carter, John Thomason, and Roger Fry for the discovery and excavation of DMNH 2013-07-1942 (“The Flying Turtle”). We thank Ty Leslie Goble and his family for discovering and donating HMNS-10-TM (“Ruby”) to the Heard Museum, where it is currently displayed. We especially recognize the hard work, patience, and talent of Patrick and Margie Kline, as well as other preparators at the Perot and Heard Museums, most of whom are volunteers. Their energy, effort and dedication made the current study possible by preparing the most complete specimens known of the newly combined taxon. We thank Dr. Dori Contreras, Brad Carter, and Murray Cohen for assistance locating the discovery site of HMNS-10-TM. We appreciate the assistance of Dr. Andrew Lee, Dr. Ari Grossman, and Avery Williams (Midwestern University) for assistance with histological thin-section preparation and logistical support. We are also grateful for the thoughtful feedback of Joshua Lively, Juliana Sterli, Christian Kammerer, and an anonymous reviewer.

REFERENCES

Adams, R.L. and Carr, J.P. 2010. Regional depositional systems of the Woodbine, Eagle Ford, and Tuscaloosa of the U. S. Gulf Coast. Gulf Coast Association of Geological Societies Transactions, 60:3-27.

Adams, T.L., Noto, C.R., and Drumheller, S. 2017. A large neosuchian crocodyliform from the Upper Cretaceous (Cenomanian) Woodbine Formation of North Texas. Journal of Vertebrate Paleontology, 37:e1349776. https://doi.org/10.1080/02724634.2017.1349776

Adrian, B., Smith, H.F., Noto, C.R., and Grossman, A. 2019. A new baenid, *"Trinitichelys" maini* sp. nov., and other fossil turtles from the Upper Cretaceous Arlington Archosaur Site (Woodbine Formation, Cenomanian), Texas, USA. Palaeontologia Electronica, 22.3.81:1-29. https://doi.org/10.26879/1001

Adrian, B., Smith, H.F., Noto, C.R., and Grossman, A. 2021. An early bothremydid from the Arlington Archosaur Site of Texas. Scientific Reports, 11, 9555. https://doi.org/10.1038/s41598-021-88905-1

Adrian, B., Smith, H.F., Kelley, K., and Wolfe, D.G. 2023. A new baenid, *Edowa zuniensis* gen. et sp. nov., and other fossil turtles from the Upper Cretaceous Moreno Hill Formation (Turonian), New Mexico, USA. Cretaceous Research, 144, 105422. https://doi.org/10.1016/j.cretres.2022.105422

Akinlotan, O. 2019. Sideritic ironstones as indicators of depositional environments in the Weald Basin (Early Cretaceous) SE England. Geological Magazine, 156:533-546. https://doi.org/10.1017/S0016756817001017

Ambrose, W.A., Hentz, T.F., Bonnaffe, F., Loucks, R.G., Brown, L.F.J., Wang, E.P., and Potter, E.C. 2009. Sequence-stratigraphic controls on complex reservoir architecture of highstand fluvial-dominated deltaic and lowstand valley-fill deposits in the Upper Cretaceous (Cenomanian) Woodbine Group, East Texas field: Regional and local perspectives. AAPG Bulletin, 93:231-269. https://doi.org/10.1306/09180808053

Archibald, D.J. 1977. Fossil Mammalia and Testudines of the Hell Creek Formation, and the Geology of the Tullock and Hell Creek Formations, Garfield County. Unpublished PhD Thesis, University of California, Berkeley.

Archibald, D.J. and Hutchison, J.H. 1979. Revision of the genus *Palatobaena* (Testudines, Baenidae), with the description of a new species. Postilla, 177:1-19.

Avrahami, H.M., Gates, T.A., Heckert, A.B., Makovicky, P.J., and Zanno, L.E. 2018. A new microvertebrate assemblage from the Mussentuchit Member, Cedar Mountain Formation: insights into the paleobiodiversity and paleobiogeography of early Late Cretaceous ecosystems in western North America. PeerJ, 6:e5883. https://doi.org/10.7717/peerj.5883

Baur, G. 1887. Über den Ursprung der Extremitäten der Ichthyopterygia. Berichte über die Versammlungen des Oberrheinischen Geologischen Vereines, 20:17-20.

Behrensmeyer, A.K. 1978. Taphonomic and ecologic information from bone weathering. Paleobiology, 4:150-162.
Berquist, H.R. 1949. Geology of the Woodbine Formation of Cooke, Grayson, and Fannin Counties, Texas. Oil and Gas Inventory Preliminary Map OM-98, USGS.
Blakey, R.C. 2014. Paleogeography and paleotectonics of the Western Interior Seaway, Jurassic-Cretaceous of North America. Search and Discovery, 30392:1-17.
Blakey, R.C. and Ranney, W.D. 2018. Ancient landscapes of western North America: A geologic history with paleogeographic maps. Springer, Berlin.
Brand, L.R., Hussey, M., and Taylor, J. 2003. Taphonomy of freshwater turtles: decay and disarticulation in controlled experiments. Journal of Taphonomy, 1:233-245.
Brinkman, D.B. 2003. Anatomy and systematics of *Plesiobaena antiqua* (Testudines; Baenidae) from the mid-Campanian Judith River Group of Alberta, Canada. Journal of Vertebrate Paleontology, 23:146-155. https://doi.org/10.1671/0272-4634(2003)23[146:aasopa]2.0.co;2
Brinkman, D.B. and Nicholls, E.L. 1991. Anatomy and relationships of the turtle *Boremys pulchra* (Testudines: Baenidae). Journal of Vertebrate Paleontology, 11:302-315. https://doi.org/10.1080/02724634.1991.10011400
Brownstein, C.D. 2018. The biogeography and ecology of the Cretaceous non-avian dinosaurs of Appalachia. Palaeontologia Electronica, 21.1.5A:1-56. https://doi.org/10.26879/801
Carpenter, K. and Bakker, R.T. 1990. A new latest Jurassic vertebrate fauna, from the highest levels of the Morrison Formation at Como Bluff, Wyoming, with comments on Morrison biochronology. Part II. A new baenid turtle. Hunteria, 2:3-4.
Cadena, E.A. 2015. The first South American sandownid turtle from the Lower Cretaceous of Colombia. PeerJ, 3:e14331. https://doi.org/10.7717/peerj.1431
Cavin, L., Toriño, P., Van Vranken, N., Carter, B., Polcyn, M.J., and Winkler, D.A. 2021. The first Late Cretaceous mawsoniid coelacanth (Sarcopterygii: Actinistia) from North America: evidence of a lineage of extinct 'living fossils'. PLoS ONE, 16:e0259292. https://doi.org/10.1371/journal.pone.0259292
Cifelli, R.L., Nydam, R.L., Gardner, J.D., Weil, A., Eaton, J.G., Kirkland, J.I., and Madsen, S.K. 1999. Medial Cretaceous vertebrates from the Cedar Mountain Formation, Emery County, Utah: The Mussentuchit local fauna, p. 219-242. In Gillette, D.D. (ed.), Vertebrate Paleontology in Utah. Utah Geological Survey, Salt Lake City.
Clark, D.L. 1965. Heteromorph ammonoids from the Albian and Cenomanian of Texas and adjacent areas. Geological Society of America Memoir, 95:1-99. https://doi.org/10.1130/MEM95
Cope, E.D. 1873. On the extinct vertebrata of the Eocene of Wyoming, observed by the expedition of 1872, with notes on the geology, p. 1-134. In Hayden, F.V. (ed.), Sixth Annual Report of the Uinted States Geological Survey of the Territories embracing portions of Montana, Idaho, Wyoming, and Utah; Being a report of progress of the explorations for the year 1872. Government Printing Office, Washington, D.C.
Cope, E.D. 1877. On reptilian remains from the Dakota beds of Colorado. Proceedings of the American Philosophical Society, 17:193-196.
Denne, R.A., Breyer, J.A., Kosanke, T.H., Spaw, J.M., Callender, A.D., Hinote, R.E., Kariminia, M., Tur, N., Kita, Z., Lees, J.A., and Rowe, H. 2016. Biostratigraphic and geochemical constraints on the stratigraphy and depositional environments of the Eagle Ford and Woodbine Groups of Texas, p. 1-86. In Breyer, J.A. (ed.), The Eagle Ford Shale: A renaissance in U.S. oil production. AAPG Memoir. https://doi.org/10.1306/13541957M1103660
Dickson, B.V. and Pierce, S.E. 2019. Functional performance of turtle humerus shape across an ecological adaptive landscape. Evolution, 73:1265-1277. https://doi.org/10.1111/evo.13747
Dodge, C.F. 1952. Stratigraphy of the Woodbine Formation in the Arlington area. Tarrant County, Texas. Field and Laboratory, 20:66-78.
Dodge, C.F. 1968. Stratigraphic nomenclature of the Woodbine Formation Tarrant County, Texas, p. 107-125. In Dodge, C.F. (ed.), Field trip Guidebook, South Central Section, Stratigraphy of the Woodbine Formation, Tarrant County, Texas. Geological Society of America, Colorado.
Dodge, C.F. 1969. Stratigraphic nomenclature of the Woodbine Formation Tarrant County, Texas. Texas Journal of Science, 21:43-62.

Donovan, A.D., Gardner, R.D., Pramudito, A., Staerker, T.S., Wehner, M., Corbett, M.J., Lundquist, J.J., Romero, A.M., Henry, L.C., Rotzien, J.R., and Boling, K.S. 2015. Chronostratigraphic relationships of the Woodbine and Eagle Ford Groups across Texas. Gulf Coast Association of Geological Societies Journal, 4:67-87.

Eaton, J.G., Cifelli, R.L., Hutchison, J.H., Kirkland, J.I., and Parrish, J.M. 1999. Cretaceous vertebrate faunas from the Kaiparowits Plateau, south-central Utah, p. 345-353. In Gillette, D.D. (ed.), Vertebrate Paleontology in Utah. Utah Geological Survey Miscellaneous Publication, Salt Lake City, UT.

Emerson, B.L., Emerson, J.H., Akers, R.E., and Akers, T.J. 1994. Texas Cretaceous ammonites and nautiloids. Houston Gem and Mineral Society, Houston, TX.

Evers, S.W., Rollot, Y., and Joyce, W.G. 2020. Cranial osteology of the Early Cretaceous turtle *Pleurosternon bullocki* (Paracryptodire: Pleurosternidae). PeerJ, 8:e9454. https://doi.org/10.7717/peerj.9454

Evers, S.W., Rollot, Y., and Joyce, W.G. 2021. New interpretation of the cranial osteology of the Early Cretaceous turtle *Arundelemys dardeni* (Paracryptodira) based on a CT-based re-evaluation of the holotype. PeerJ, 9:e11495. https://doi.org/10.7717/peerj.11495

Fiorillo, A.R., Padian, K., and Musikasinthorn, C. 2000. Taphonomy and depositional setting of the *Placerias* Quarry (Chinle Formation: Late Triassic, Arizona). Palaios, 15:373-386. https://doi.org/10.1669/0883-1351(2000)015%3C0373:TADSOT%3E2.0.CO;2

Gaffney, E.S. 1972. The systematics of the North American family Baenidae (Reptilia, Cryptodira). Bulletin of the American Museum of Natural History, 147:1-84.

Gaffney, E.S. 1990. The comparative osteology of the Triassic turtle *Proganochelys*. Bulletin of the American Museum of Natural History, 194:1-263.

Gaffney, E.S. and Hiatt, R. 1971. A new baenid turtle from the Upper Cretaceous of Montana. American Museum Novitates, 2443:1-9.

Gaffney, E.S., and Meylan, P.A. 1988. A phylogeny of turtles. In Benton, M.J. (ed.), The phylogeny and classification of the tetrapods, Volume 1: Amphibians, Reptiles, Birds. Systematics Association Special Volume. Clarendon Press, Oxford.

Gilmore, C.W. 1915. The fossil turtles of the Uinta Formation. Memoirs of the Carnegie Museum, 7:101-162.

Gilmore, C.W. 1916. Contributions to the geology and paleontology of San Juan County, New Mexico. 2. Vertebrate faunas of the Ojo Alamo, Kirtland, and Fruitland formations. United States Geological Survey Professional Paper, 98:279-308.

Gilmore, C.W. 1920. New fossil turtles, with notes on two described species. Proceedings of the United States National Museum, 56:113-132. https://doi.org/10.5479/si.00963801.56-2292.113

Gilmore, C.W. 1935. On the Reptilia of the Kirtland Formation of New Mexico, with descriptions of new species of fossil turtles. Proceedings of the United States National Museum, 83:159-188. https://doi.org/10.5479/si.00963801.83-2978.159

Goloboff, P.A. and Morales, M. 2023. TNT version 1.6, with a graphical interface for MacOS and Linux, including new routines in parallel. Cladistics, 39:144-153. https://doi.org/10.1111/cla.12524

Goloboff, P.A., Torres, A., and Arias, J.S. 2018. Weighted parsimony outperforms other methods of phylogenetic inference under models appropriate for morphology. Cladistics, 34:407-437. https://doi.org/10.1111/cla.12205

Gradstein, F.M., Ogg, J.G., and Smith, A.G. 2004. A geologic time scale 2004. Cambridge University Press, UK.

Hay, O.P. 1901. Description of a new species of *Baëna* (*B. hatcheri*) from the Laramie Beds of Wyoming. Annals of the Carnegie Museum, 1:325-326. https://doi.org/10.5962/p.331061

Hay, O.P. 1904. On some fossil turtles belonging to the Marsh collection in Yale University Museum. American Journal of Science, 18:261-276. https://doi.org/10.2475/ajs.s4-18.106.261

Hay, O.P. 1908. The Fossil Turtles of North America. Carnegie Institute of Washington, Washington D.C.

Head, J.J. 1998. A new species of basal hadrosaurid (Dinosauria, Ornithischia) from the Cenomanian of Texas. Journal of Vertebrate Paleontology, 18:718-738. https://doi.org/10.1080/02724634.1998.10011101

Hentz, T.F., Ambrose, W.A., and Smith, D.C. 2014. Eaglebine play of the southwestern East Texas Basin: stratigraphic and depositional framework of the Upper Cretaceous (Cenomanian-Turonian) Woodbine and Eagle Ford Groups. American Association of Petroleum Geologists Bulletin, 98:2551-2580. https://doi.org/10.1306/07071413232

Holroyd, P.A. and Hutchison, J.H. 2002. Patterns of geographic variation in latest Cretaceous vertebrates: evidence from the turtle component. Geological Society of America Special Papers, 361:177-190. https://doi.org/10.1130/0-8137-2361-2.177

Holroyd, P.A., Wilson, G.P., and Hutchison, J.H. 2014. Temporal changes within the latest Cretaceous and early Paleogene turtle faunas of northeastern Montana, p. 299-312. In Wilson, G.P., W.A.Clemens, W.A., Horner, J.R., and Hartman, J.H. (eds.), Through the end of the Cretaceous in the type locality of the Hell Creek Formation in Montana and adjacent areas: Geological Society of America Special Paper. https://doi.org/10.1130/2014.2503(11)

Hutchison, J.H. 1984. Determinate growth in the Baenidae (Testudines): taxonomic, ecologic, and stratigraphic significance. Journal of Vertebrate Paleontology, 3:148-151. https://doi.org/10.1080/02724634.1984.10011968

Hutchison, J.H. 2004. A new Eubaenine, *Goleremys mckennai,* gen. et sp. n., (Baenidae: Testudines) from the Paleocene of California. Bulletin of the Carnegie Museum of Natural History, 36:91-96. https://doi.org/10.2992/0145-9058(2004)36[91:anegmg]2.0.co;2

Hutchison, J.H., and Bramble, D.M. 1981. Homology of the Plastral Scales of the Kinosternidae and Related Turtles. Herpetologica, 37:73-85.

Hutchison, J.H. and Storer, J.E. 1998. Turtles from the middle Eocene (Uintan) of Saskatchewan, Canada. Paleobios, 18:36-39.

Hutchison, J.H., Knell, M.J., and Brinkman, D.B. 2013. Turtles from the Kaiparowits Formation, Utah, p. 295-318. In Titus, A.L. and Loewen, M.A. (eds.), At the top of the Grand Staircase: The Late Cretaceous of Southern Utah. Indiana University Press, Bloomington.

Jacobs, L.L. and Winkler, D.A. 1998. Mammals, archosaurs, and the Early to Late Cretaceous transition in north-central Texas. National Science Museum Monographs, 14:253-280.

Jacobs, L.L., Polcyn, M.J., Winkler, D.A., Myers, T.S., Kennedy, J.G., and Wagner, J.B. 2013. Late Cretaceous strata and vertebrate fossils of North Texas, p. 1-13, Late Cretaceous to Quaternary strata and fossils of Texas: field excursions celebrating 125 years of GSA and Texas geology, GSA South-Central Section Meeting, Austin, Texas, April 2013. Geological Society of America, Austin, TX. https://doi.org/10.1130/2013.0030(01)

Johnson, R.O. 1974. Lithofacies and depositional environments of the Rush Creek Member of the Woodbine Formation (Gulfian) of north central Texas. Unpublished MS Thesis, University of Texas, Arlington.

Joyce, W.G. 2007. Phylogenetic relationships of Mesozoic turtles. Bulletin of the Peabody Museum of Natural History, 48:3-102. https://doi.org/10.3374/0079-032X(2007)48[3:PROMT]2.0.CO;2

Joyce, W.G. 2017. A review of the fossil record of basal Mesozoic turtles. Bulletin of the Peabody Museum of Natural History, 58:65-113. https://doi.org/10.3374/014.058.0105

Joyce, W.G. and Lyson, T.R. 2015. A review of the fossil record of turtles of the clade *Baenidae*. Bulletin of the Peabody Museum of Natural History, 56:147-183. https://doi.org/10.3374/014.056.0203

Joyce, W.G., Rollot, Y., and Cifelli, R.L. 2020. A new species of baenid turtle from the Early Cretaceous Lakota Formation of South Dakota. Fossil Record, 23:1-13. https://doi.org/10.5194/fr-23-1-2020

Joyce, W.G., Anquetin, J., Cadena, E.-A., Claude, J., Danilov, I.C., Evers, S.W., Ferreira, G.S., Gentry, A.D., Georgialis, G., Lyson, T.R., Pérez-García, A., Rabi, M., Sterli, J., Vitek, N.S., and Parham, J.F. 2021. A nomenclature for fossil and living turtles using phylogenetically defined clade names. Swiss Journal of Palaeontology, 140:1-45. https://doi.org/10.1186/s13358-020-00211-x

Kennedy, W.J. and Cobban, W.A. 1990. Cenomanian ammonite faunas from the Woodbine Formation and lower part of the Eagle Ford Group, Texas. Palaeontology, 33:75-154.
Kline, P., Kline, M., and Main, D.J. 2012. Mapping and lab preparation of a Cretaceous (Cenomanian) turtle from the Woodbine Formation of North Texas: the unusual challenges of the Flying Turtle Project. Journal of Vertebrate Paleontology Program and Abstracts 2012, 122. Raleigh, NC.
Lambe, L.M. 1902. New genera and species from the Belly River Series (mid-Cretaceous). Contributions to Canadian Paleontology, 3:25-81. https://doi.org/10.5281/zenodo.3233762
Lambe, L.M. 1906. Description of new species of *Testudo* and *Baëna* with remarks on some Cretaceous forms. Ottawa Naturalist, 19:232-234.
Larson, D.W., Longrich, N.R., Evans, D.C., and Ryan, M.J. 2013. A new species of *Neurankylus* from the Milk River Formation (Cretaceous: Santonian) of Alberta, Canada, and a revision of the type species *N. eximius*, p. 389-405. In Brinkman, D.B., Holroyd, P.A., and Gardner, J.D. (ed.), Morphology and Evolution of Turtles. Springer Science + Business Media, Dordrecht. https://doi.org/10.1007/978-94-007-4309-0_21
Latreille, P.A. 1801. Histoire Naturelle des Reptiles, p. 280. In Sonnini, C.S. and Latreille, P.A. (eds.), Histoire naturelle des reptiles, avec figures dessinées d'après nature. Tome premier. Première Partie. Quadrupèdes et Bipèdes Ovipares. Détérville, Paris, https://doi.org/10.5962/bhl.title.4277
Laurin, M., de Queiroz, K., Cantino, P., Cellinese, N., and Olmstead, R. 2005. The PhyloCode, type, ranks, and monophyly: a response to Pickett. Cladistics, 21:605-607. https://doi.org/10.1111/j.1096-0031.2005.00090.x
Lee, Y.-N. 1997. The Archosauria from the Woodbine Formation (Cenomanian) in Texas. Journal of Paleontology, 71:1147-1156. https://doi.org/10.1017/S0022336000036088
Lee, A.H. and Simons, E.L.R. 2015. Wing bone laminarity is not an adaptation for torsional resistance in bats. PeerJ, 3:e823. https://doi.org/10.7717/peerj.823
Leidy, J. 1870. [Descriptions of *Emys jeansi*, *Emys haydeni*, *Baena arenosa*, and *Saniwa ensidens*]. Proceedings of the Academy of Natural Sciences of Philadelphia, 1870:123-124.
Leidy, J. 1871a. [Remarks on some extinct turtles from Wyoming Territory]. Proceedings of the Academy of Natural Sciences of Philadelphia, 1871:102-103.
Leidy, J. 1871b. Report on the vertebrate fossils of the Tertiary formations of the West. Preliminary Report of the United States Geological Survey of Wyoming and Portions of Contiguous Territories, 4:340-370.
Lichtig, A.J. and Lucas, S.G. 2015. Cretaceous turtles of New Mexico. New Mexico Museum of Natural History and Science Bulletin, 67:129-137.
Lichtig, A.J. and Lucas, S.G. 2016. A new species of *Neurankylus* (Testudines: Baenidae) from the Upper Cretaceous Crevasse Canyon Formation, southern New Mexico, USA. New Mexico Museum of Natural History and Science Bulletin, 74:117-119.
Lichtig, A.J. and Lucas, S.G. 2017. Sutures of the shell of the Late Cretaceous-Paleocene baenid turtle *Denazinemys*. Neues Jahrbuch für Geologie und Paläontologie - Abhandlungen, 283:1-8. https://doi.org/10.1127/njgpa/2017/0622
Lichtig, A.J. and Lucas, S.G. 2018. *Neurankylus*, a Cretaceous-Paleocene baenid turtle from North America. New Mexico Museum of Natural History and Science Bulletin, 79:323-361.
Lipka, T.R., Therrien, F., Weishampel, D.B., Jamniczky, H.A., Joyce, W.G., Colbert, M.W., and Brinkman, D.B. 2006. A new turtle from the Arundel Clay facies (Potomac Formation, Early Cretaceous) of Maryland, U.S.A. Journal of Vertebrate Paleontology, 26:300-307. https://www.jstor.org/stable/4524570
Lively, J.R. 2015. A new species of baenid turtle from the Kaiparowits Formation (Upper Cretaceous, Campanian) of southern Utah. Journal of Vertebrate Paleontology, 35:e1009084. https://doi.org/10.1080/02724634.2015.1009084
Lively, J.R. 2016. Baenid turtles of the Kaiparowits Formation (Upper Cretaceous: Campanian) of southern Utah, USA. Journal of Systematic Palaeontology, 14:891-918. https://doi.org/10.1080/14772019.2015.1120788

Lyson, T.R. and Joyce, W.G. 2009a. A revision of *Plesiobaena* (Testudines: Baenidae) and an assessment of baenid ecology across the K/T boundary. Journal of Paleontology, 83:833-853.
https://doi.org/10.1666/09-035.1

Lyson, T.R. and Joyce, W.G. 2009b. A new species of *Palatobaena* (Testudines: Baenidae) and a maximum parsimony and bayesian phylogenetic analysis of Baenidae. Journal of Paleontology, 83:457-470.
https://doi.org/10.1666/08-172.1

Lyson, T.R. and Joyce, W.G. 2010. A new baenid turtle from the Upper Cretaceous (Maastrichtian) Hell Creek Formation of North Dakota and a preliminary taxonomic review of Cretaceous Baenidae. Journal of Vertebrate Paleontology, 30:394-402.
https://doi.org/10.1080/02724631003618389

Lyson, T.R. and Joyce, W.G. 2011. Cranial anatomy and phylogenetic placement of the enigmatic turtle *Compsemys victa* Leidy, 1856. Journal of Paleontology, 85:786-801.
https://doi.org/10.1666/10-081.1

Lyson, T.R., Joyce, W.G., Knauss, G.E., and Pearson, D.A. 2011. *Boremys* (Testudines: Baenidae) from the Latest Cretaceous and Early Paleocene of North Dakota: an 11-million-year range extension and an additional K/T survivor. Journal of Vertebrate Paleontology, 31:729-737.
https://doi.org/10.1080/02724634.2011.576731

Lyson, T.R., Joyce, W.G., Lucas, S.G., and Sullivan, R.M. 2016. A new baenid turtle from the early Paleocene (Torrejonian) of New Mexico and a species-level phylogenetic analysis of Baenidae. Journal of Paleontology, 90:305-316.
https://doi.org/10.1017/jpa.2016.47

Lyson, T.R., Sayler, J.L., and Joyce, W.G. 2019. A new baenid turtle, *Saxochelys gilberti*, gen. et sp. nov., from the uppermost Cretaceous (Maastrichtian) Hell Creek Formation: Sexual dimorphism and spatial niche partitioning within the most speciose group of Late Cretaceous turtles. Journal of Vertebrate Paleontology, 39:e1662428.
https://doi.org/10.1080/02724634.2019.1662428

Lyson, T.R., Petermann, H., Toth, N., Bastien, S., and Miller, I.M. 2021. A new baenid turtle, *Palatobaena knellerorum* sp. nov., from the lower Paleocene (Danian) Denver Formation of south-central Colorado, U.S.A. Journal of Vertebrate Paleontology, 41:e1925558.
https://doi.org/10.1080/02724634.2021.1925558

Main, D.J. 2005. Paleoenvironments and Paleoecology of the Cenomanian Woodbine Formation of Texas: Paleobiogeography of the Hadrosaurs (Dinosauria: Ornithischia). Unpublished MS Thesis, University of Texas, Arlington, Arlington.

Main, D.J. 2009. Delta plain environments and ecology of the Cretaceous (Cenomanian) Woodbine Formation at the Arlington Archosaur Site, North Texas. Geological Society of America Abstracts with Programs, 41(103).

Main, D.J., Noto, C.R., and Scotese, C.R. 2010. Coastal Cretaceous forest fires, paleosols, dinosaur paleoecology from the Arlington Archosaur Site, North Texas. Geological Society of America Abstracts with Programs, 42(5):175.

Main, D.J., Parris, D.C., Grandstaff, B.G., and Carter, B. 2011. A new lungfish (Dipnoi: Ceratodontidae) from the Cretaceous Woodbine Formation, Arlington Archosaur Site, North Texas. Texas Journal of Science, 63:283-298.

Main, D.J. 2013. Appalachian delta plain paleoecology of the Cretaceous Woodbine Formation at the Arlington Archosaur Site, North Texas. Unpublished PhD Thesis, The University of Texas, Arlington.

Main, D.J., Noto, C.R., and Weishampel, D.B. 2014. Postcranial anatomy of a basal hadrosauroid (Dinosauria: Ornithopoda) from the Cretaceous (Cenomanian) Woodbine Formation of north Texas, p. 77-95. In Eberth, D.A. and Evans, D.C. (eds.), Hadrosaurs. Indiana University Press, Bloomington.

Murlin, J.R. 1975. Stratigraphy and depositional environments of the Arlington Member, Woodbine Formation (Upper Cretaceous), Northeast Texas. Unpublished MS Thesis, University of Texas at Arlington, Arlington, TX.

Nakajima, Y., Hirayama, R., and Endo, H. 2014. Turtle humeral microanatomy and its relationship to lifestyle. Biological Journal of the Linnean Society, 112:719-734.
https://doi.org/10.1111/bij.12336

Noto, C.R. 2015. Archosaur localities in the Woodbine Formation (Cenomanian) of North Central Texas. Early- and mid-Cretaceous archosaur localities in north-central Texas. Fieldtrip Guidebook, Society of Vertebrate Paleontology Annual Meeting:38-51.

Noto, C.R., Main, D.J., and Drumheller, S.K. 2012. Feeding traces and paleobiology of a Cretaceous (Cenomanian) crocodyliform: example from the Woodbine Formation of Texas. Palaios, 27:105-115. https://doi.org/10.2110/palo.2011.p11-052r

Noto, C.R., Drumheller, S., Adams, T.L., and Turner, A.H. 2019. An enigmatic small neosuchian crocodyliform from the Woodbine Formation of Texas. The Anatomical Record, 302:802-812. https://doi.org/10.1002/ar.24174

Noto, C.R., D'Amore, D.C., Drumheller, S.K., and Adams, T.L. 2022. A newly recognized theropod assemblage from the Lewisville Formation (Woodbine Group; Cenomanian) and its implications for understanding Late Cretaceous Appalachian terrestrial ecosystems. PeerJ, 10:e12782. https://doi.org/10.7717/peerj.12782

Oliver, W.B. 1971. Depositional systems in the Woodbine Formation (Upper Cretaceous), northeast Texas: The University of Texas at Austin. Bureau of Economic Geology Report of Investigations, 73:28.

Pfretzschner, H.-U. 2004. Fossilization of Haversian bone in aquatic environments. Comptes Rendus Palevol, 3:605-616. https://doi.org/10.1016/j.crpv.2004.07.006

Powell, J.D. 1968. Woodbine-Eagle Ford transition, Tarrant Member, p. 27-43. In Dodge, C.F. (ed.), Stratigraphy of the Woodbine Formation: Tarrant County, Texas Field Trip Guidebook. Geological Society of America, South Central Section, Denver.

Pritchard, P.C.H. (1966). Occurrence of Mesoplastra in a Cryptodiran Turtle, *Lepidochelys olivacea*. Nature, 210:652. https://doi.org/10.1038/210652a0

Rabenhorst, M.C. 2001. Soils of tidal and fringing wetlands. In Richardson, J.L., Vepraskas, M.J. and Craft, C.B. (eds.), Wetland soils: Genesis, hydrology, landscapes, and classification. Lewis Publishers, Boca Raton.

Rasband, W.S. 1997-2018. ImageJ. Bethesda, MD, USA, U.S. National Institutes of Health.

Reeside, J.J.B. and Cobban, W.A. 1960. Studies of the Mowry Shale (Cretaceous) and contemporary formations in the United States and Canada. United States Geological Survey Professional Paper, 355:1-126.

Rollot, Y., Evers, S.W., and Joyce, W.G. 2021. A redescription of the Late Jurassic (Tithonian) turtle *Uluops uluops* and a new phylogenetic hypothesis of *Paracryptodira*. Swiss Journal of Palaeontology, 140:1-30. https://doi.org/10.1186/s13358-021-00234-y

Rollot, Y., Evers, S.W., Cifelli, R.L., and Joyce, W.G. 2022a. New insights into the cranial osteology of the Early Cretaceous paracryptodiran turtle *Lakotemys australodakotensis*. PeerJ, 10:e13230. https://doi.org/10.7717/peerj.13230

Rollot, Y., Evers, S.W., Pierce, S.E., and Joyce, W.G. 2022b. Cranial osteology, taxonomic reassessment, and phylogenetic relationships of the Early Cretaceous (Aptian-Albian) turtle *Trinitichelys hiatti* (Paracryptodira). PeerJ, 10, e14138. https://doi.org/10.7717/peerj.14138

Russell, L.S. 1934. Fossil turtles from Saskatchewan and Alberta. Proceedings and Transactions of the Royal Society of Canada, 28(4):101-112.

Scheyer, T.M. 2007. Comparative bone histology of the turtle shell (carapace and plastron): implications for turtle systematics, functional morphology and turtle origins. Unpublished PhD Thesis, University of Bonn.

Schoepff, J.D. 1793. Historia Testudinum Iconibus Illustrata. Ioannis Iacobi Palm, Erlangae.

Schwimmer, D.R. 1997. Late Cretaceous dinosaurs in Eastern USA: A taphonomic and biogeographic model of occurrences, p. 203-211. In Wolberg, E. and Stump, E. (eds.), Dinofest International Proceedings. Philadelphia Academy of Natural Sciences, Philadelphia, Pennsylvania.

Scotese, C.R. 2021. An atlas of Phanerozoic Paleogeographic Maps: the seas come in and the seas go out. Annual Review of Earth and Planetary Sciences, 49:679-728. https://doi.org/10.1146/annurev-earth-081320-064052

Selley, R.C., Cocks, L.R.M., and Plimer, I.R. 2005. Encyclopedia of Geology. Amsterdam, Elsevier.

Slattery, J.S., Cobban, W.A., McKinney, K.C., Harries, P.J., and Sandness, A.L. 2015. Early Cretaceous to Paleocene paleogeography of the Western Interior Seaway: the interaction of eustasy and tectonism, p. 22-60. In Bingle-Davis, M. (ed.), Wyoming Geological Association Guidebook. Wyoming Geological Association, Casper.

Smith, H.F., Hutchison, H.J., Townsend, B.K.E., Adrian, B., and Jager, D. 2017. Morphological variation, phylogenetic relationships, and geographic distribution of the Baenidae (Testudines), based on new specimens from the Uinta Formation (Uinta Basin), Utah (USA). PLoS ONE, 12:e0180574. https://doi.org/10.1371/journal.pone.0180574

Stephenson, L.W. and Stenzel, H.B. 1952. Larger invertebrate fossils of the Woodbine Formation (Cenomanian) of Texas, with decapod crustaceans from the Woodbine Formation of Texas USGS Professional Paper, 242:1-225. https://doi.org/10.3133/pp242

Sullivan, R.M., Jasinkski, S.E., and Lucas, S.G. 2013. Re-Assessment of Late Campanian (Kirtlandian) turtles from the Upper Cretaceous Fruitland and Kirtland Formations, San Juan Basin, New Mexico, p. 337-386. In Brinkman, D.B., Gardner, J.D., and Holroyd, P.A., (eds.), Morphology and Evolution of Turtles. Springer Science & Business Media, Dordrecht. https://doi.org/10.1007/978-94-007-4309-0_20

Thurmond, J.T. 1974. Lower vertebrate faunas of the Trinity Division in North-Central Texas. Geoscience and Man, 8:103-129.

Trudel, P. 1994. Stratigraphic sequences and facies architecture of the Woodbine-Eagle Ford interval, Upper Cretaceous, North Central Texas. Unpublished MS Thesis, Tarleton State University.

Tykoski, R.S. and Fiorillo, A.R. 2010. An entantiornithine bird from the lower middle Cenomanian of Texas. Journal of Vertebrate Paleontology, 30:288-292.

Vallabhaneni, S., Olszewski, T.D., Pope, M.C., and Heidari, Z. 2016. Facies and stratigraphic interpretation of the Eaglebine Play in Central Texas. Gulf Coast Association of Geological Societies Journal, 5:25-46.

Williams, E.E. 1950. Variation and selection in the cervical central articulations of living turtles. Bulletin of the American Museum of Natural History, 94(9):507-561. https://doi.org/10.1086/399607

Winkler, D., Jacobs, L., Lee, Y., and Murry, P. 1995. Sea level fluctuation and terrestrial faunal change in North-Central Texas. In Sun, A. and Wang, Y. (eds.), Sixth Symposium on Mesozoic Terrestrial Ecosystems and Biota. China Ocean Press, Beijing.

Zanno, L.E. and Makovicky, P.J. 2013. Neovenatorid theropods are apex predators in the Late Cretaceous of North America. Nature Communications, 4:2827. https://doi.org/10.1038/ncomms3827

Zanno, L.E., Tucker, R.T., Canoville, A., Avrahami, H.M., Gates, T.A., and Makovicky, P.J. 2019. Diminutive fleet-footed tyrannosauroid narrows the 70-million-year-gap in the North American fossil record. Communications Biology, 2:64. https://doi.org/10.1038/s42003-019-0308-7

APPENDIX 1.

Measurements of *Gehennachelys maini* comb. nov. Measurements are in cm and are estimated if preceded by a tilde (~).

	DMNH 2013-07-1942	HMNS-10-TM	DMNH 2013-07-0784	DMNH 2013-07-1711	DMNH 2013-07-0712
Carapace					
Length	47.5	38.9	~27.2	—	—
Width	40.8	34.3	—	—	—
Height	—	11.4	—	—	—
Cervical scale					
Length	—	—	1.6	1.0	—
Width	—	—	4.4	1.9	—
Vertebral scales					
1 Length	—	—	4.0	—	—
Width	—	—	8.1	—	—
2 Length	—	—	~6.7	—	—
Width	—	—	~10.4	—	—
5 Length	—	—	4.2	—	—
Width	—	—	5.9	—	—
Plastron length	—	36.3	—	—	—
Bridge length	—	18.3	—	—	—
Anterior lobe					
Length	—	8.3	—	—	~8.1
Width	16.5	13.1	—	—	~14.4
Median gular contact	—	—	—	—	3.0
Median extragular contact	—	—	—	—	0.9
Posterior lobe					
Length	11.5	10.5	—	—	—
Width	15.6	13.0	—	—	—

APPENDIX 2.

Phylogenetic coding for *Gehennachelys maini* comb. nov. using the character matrix described in Phylogenetic Methods above from Rollot et al. (2022b), with parentheses indicating polymorphic states:

Gehennachelys maini comb. nov 00??????10 ?0?11???01 1????????? ?100??0100 0000101010 0????0??00 100????1?? 111??10000 (0&1)11112????1 ?0?02????? ?0100

SUPPLEMENTARY DATA

Character-taxon matrix for the phylogenetic analysis performed in this study (TNT format; Goloboff and Morales 2023). Missing data are coded as "?", and polymorphic character states are in brackets. Character matrix modified from Rollot et al. (2022b).

```
xread
105 50
            Proganochelys_quenstedti
0000000000000000000-000-
000000000000100??1100000000000000000
1000000000000000?00000????????0?0000
?000-0
            Kayentachelys_aprix
00000000[0 1]0000010?0?0-000-
000001000000100000100000000000000000
1000101000000000000000??001010000000
?00000
            Eileanchelys_waldmani
0000??0?10100010000??1??0?0?0?000?00
10000020?00?000?00010010??001?????0?
??11000?????010??10001000?10000

Sichuanchelys_palatodentata
10002000?00000000010-
?101???0?1000000100000l?2000000000000
100001000?001[0
1]????00000????????1?10000000000000
            Mongolochelys_efremovi
1000000001000000000-
0?0110?001001?011000001000000000000
00101100000010O???00000????1010[0
1]0100011?00?0000
            Chubutemys_copelloi
0000200010?0000000?0???1100??????1002
?000001?????0000000000?10?100??????0?
?????00?00?0?0101?10?000?00?000?
            Peligrochelys_walshae
????10???0?0000?00?????????????????
1?0??????????0????0?0?00????00??00???0
??0??0????????????1????1?0???0?0
            Dinochelys_whitei
?000?0?0?0?00010???0?????????0?000000
1000001?10100000000?00??00101?110????0
0?10000?00010??11110???????0?0?
            Glyptops_ornatus
10002001?0?00?102?000100020000000000
1100001010000000000000?001011110100?
00110001000101011110?1?00?10000
            Uluops_uluops
0000100110000010010000?11200?????????
?????????????0000001002011?1???010?
??1?????????????????0111001???0
            Pleurosternon_bullockii
1000200?10000010210001000[1
2]00???000[01]0000000010[0
1]000000000?10010011011??000?0011001
?0001010101[1 2]01111O1?0000
            Pleurosternon_moncayensis
????????????????????01?????200?????????
????????0?0?????0???0?0??01?????????
??11?????????????????1110110??0
            Dorsetochelys_typocardium
10002001?00000101?0001?0220????000000
1100001?10000000000000020011011???1??
??11000????10101112O0?1???10000
            Riodevemys_inumbragigas
??????????????????????????????????000001
1000001?100000?????????????????????????
???1000??0?10101012l????????0?0?
            Toremys_cassiopeia
????????????????????????????????????000000
0?00001?100000?????????????????????????
???1001??0?10?010120????????000?
            Helochelydra_nopcsai
1?0021-010?000202100-
0?032000000?0??0?????????????0?010?000
0120010001011[0
1]10??12???0000???????0?0?10???11?0
            Naomichelys_speciosa
110[0 1]????00000?202[0 1]00-
0???1??000000000?0010011?000000?00000
?1100?0010?1111??11200000002010101000
?10??11100
            Aragochersis_lignitesta
??0??????????2?????????????????000000
1000001110000??0?000???0??0????1????
?1120000000201010110O?1????1100
            Kallokibotion_bajazidi
01000?0?100000100010-
01?230??0100000100000021100000?00000
?000110001?01[0
1]0??00101000011?0100?11001000010011
            Compsemys_victta
0100100100000000010?0?023?0???000000
0100002120000000000000?0010100??100?
??0101110111000012l?200???0011
            Berruchelus_russelli
????????????????????????????????000000
0?000021200000?????????????????????????
???1?11??1110?0001[1 2]1???????00??
            Peltochelys_duchastelli
????????????????????????????????????000102
```

```
?100002?10000?????????????????????????
???1010??1?10100112?????????000?
            Selenemys_lusitanica
?????????????????????????????????000000
00000021100000?????????????????????????
???1010??1??01000121???????0?0?
            Trinitichelys_hiatti
1000100110100010200011002 3?0?????00?0
1000?0110000?00000000001011100 0??000?
?01110?1011??1????10220?0110??0
            Arundelemys_dardeni
000010010000001020????00230[0
1]?????????????????????????00000000??0?
11010??000???1?????????????????????20001
1???0

Lakotemys_australodakotensis
1000?0?0101000202000 11?11300???000?00
?1???0?11000?00000000001011 1?1????0??
???10?01111101 0?1?10220100?0000
            Arvinachelys_goldeni
0100110100000 00?2101 1?1 13?1?1?210???
100000??0111100000012 00?011100010011?
????0?1??11??11???10220????0??0
            Neurankylus_exemius
0?70??0??0000?10???001??1[2
3]?1?0?1000001100001110000000000010100
001?000100?1111001001011101110110[1
2]201??00000
            Neurankylus_torrejonensis
000?????00000010 1??0???0?3????0?100???
110000?110???00?0????00?001?0001001??
??00??0??11????????0??0????0???
            Hayemys_latifrons
00????0??0000?012?0111?113?0?????????
?????????????000000000?0011000??011?
???0???0?????????????120????????0
            Plesiobaena_antiqua
0000110110[0 1][0
2]10112001111013000101111010110000010 1
111000000000010011001011111110000011 1
100111-00022010100000
            Peckemys_brinkman
00000101[0 1]01?1[0 1]111[0
1]0100102310011 1??0101000011 01??1000
000120010 0?????????????????01111?????
???0220?010??00
            Cedrobaena_putorius
000011111 1??11111[0 1]01111[0
1]2?1001?????????????????????????00000000
1010?????????????????????????????????22
0???0??00
            Goleremys_mckennai
0000111?100020211001??10?3???????????
????????????????01000?000?0?11001??11??
??????????????????????2?0????????0
            Boremys_pulchra
0?00?11??0?01?11??0111?0??101?0210110
211111111101110000000001001100101111 1
0002000111101111-0002??1???000?
            Boremys_grandis
??????????????????????????????????210110
221111111101111?????????????????????
???2000111101 1?1?000????????000?
            Eubaena_cephalica
01011110110010[0
1]120011110131 0?????????????????????
?000000110100110 01??111???0000???????
???????2200 21????0
            Palatobaena_cohen
200021011112201 11[0
1]011110131001111 10?01100000 10?11?011
1101111[1
2]10110110 1?11???00000111 1????1??1022
0101?0000
            Palatobaena_bairdi
200021011112201100010010131001 1??????
????????????1111001112101101101?11?
??0????????????????220????????0
            Palatobaena_gaffneyi
200121010112211110010010031 0?????????
????????????1111001112101101 1???11?
??0????????????????120????????0
            Palatobaena_knellerorum
200021001112102100010010 13?0?????????
????????????1111001012101101 1???11?
??0????????????????220????????0
            Stygiochelys_estesi
001011001111211110011101031 1?????????
2211?0??01???000000100100110010111?
??000001111 1???????[1 2]20??1???00
            Saxochelys_gilberti
0010110011102[0 1]212001110[0
1]1310210[1 2]101002[1 2]1100[0
1]10101100000000001011100101100 1??010
001111011[0 1]1-0[0 1]022001110000
            Baena_arenosa
00101100[0 1]01?21110[0
1]10000013112001100112201001101111000
000000000111 0?101111???0000011 11??111
-0000200 21?0000
            Chisternon_undatum
00101100111121110[0
1]10100103112001101102211001101101000
000001010111001011111110000011 11??1?1
-000020????0000
            Gamerabaena_sonsalla
0000110011[0 1]110[0
```

```
1]120?????01?10?????????????????????
?00001?11??1?11001??1?1???0??????????
????????201???????
            Denazinemys_nodosa
??????????????????????????????????210?10
22110011110?11?????????????????????????
???20001111????1-000???????000?
            Scabremys_ornata
??????????????????????????????????110?10
11000011010?10?????????????????????????
???20001111????????0???????000?
            Edowa_zuniensis
??????????????????????????????0?00?0
01?0???101???0?????????????????????????
???0???1111?????????????????0???
```

```
            Gehennachelys_maini
00??????10?0?11???011??????????100??0
10000001010100????0??00100????1??111?
?10000[0 1]1111????1?0?02??????0100

;

ccode + 4 8 12 14 16 24 25 28 31 36
37 38 43 45 57 60 77 85 92 94 95 98;

proc /;
comments 0
;
```